SWAT-Tb with improved LAI representation in the tropics highlights the role of forests in watershed regulation

Santiago Valencia[1], Juan F. Salazar[1], Juan Camilo Villegas[1], Natalia Hoyos[2], and Mateo Duque-Villegas[3]

[1]Universidad de Antioquia
[2]Universidad del Norte
[3]Max Planck Institute

November 23, 2022

Abstract

Projecting the potential impacts of LULC (Land Use/Land Cover) change on watershed hydrological response is critical for water management decisions in a changing environment. An improved representation of vegetation dynamics is needed to improve the capability of several hydrological models to produce reliable projections of these impacts. Here we in troduce a modification in the plant growth module of SWAT (Soil Water Assessment Tool) to improve the representation of the bimodal seasonality of LAI (Leaf Area Index), which is particularly important for tropical watersheds with bimodal precipitation regimes. The new SWAT-Tb variant that we propose here reproduces not only observed streamflow, but also the bimodal seasonal pattern of LAI in a tropical mountain watershed of the Andes. In contrast, standard SWAT is inherently unable to reproduce this bimodality, although it can be calibrated to reproduce streamflow. Differences between models in the representation of LAI seasonality can lead to significantly different results about LULC change impacts on streamflow. SWAT-Tb results show that deforestation impacts on streamflow are more pronounced for seasonal than for annual streamflow, and indicate that forests can play a crucial role in enhancing water availability during dry seasons. The seasonality of streamflow anomalies is switched due to forest-to-pasture conversion, implying that while forest expansion increases water availability in dry seasons, forest conversion into pasture decreases it. Due to its poor representation of LAI seasonality, standard SWAT largely underestimates this role of forest, which can be misleading for decision making about water security and forest conservation

SWAT-Tb with improved LAI representation in the tropics highlights the role of forests in watershed regulation

Santiago Valencia[1], Juan F. Salazar[1], Juan Camilo Villegas[2], Natalia Hoyos[3], Mateo Duque-Villegas[1,4,5]

[1]GIGA, Escuela Ambiental, Facultad de Ingeniería, Universidad de Antioquia, Medellín, Colombia
[2]Grupo de investigación en Ecología Aplicada, Escuela Ambiental, Facultad de Ingeniería, Universidad de Antioquia, Medellín, Colombia
[3]Department of History and Social Sciences, Universidad del Norte, Barranquilla 080001, Colombia
[4]Max Planck Institute for Meteorology, Hamburg, Germany
[5]International Max Planck Research School on Earth System Modelling, Hamburg, Germany

Key Points:

- New SWAT (Soil and Water Assessment Tool) model variant captures bimodal tropical vegetation dynamics
- Seasonality of streamflow anomalies is switched due to forest-to-pasture conversion
- Deforestation exacerbates low flows during dry season
- Standard SWAT leads to misleading conclusion about deforestation impacts

Corresponding author: Santiago Valencia, `santiago.valencia8@udea.edu.co`

Abstract

Projecting the potential impacts of LULC (Land Use/Land Cover) change on watershed hydrological response is critical for water management decisions in a changing environment. An improved representation of vegetation dynamics is needed to improve the capability of several hydrological models to produce reliable projections of these impacts. Here we introduce a modification in the plant growth module of SWAT (Soil Water Assessment Tool) to improve the representation of the bimodal seasonality of LAI (Leaf Area Index), which is particularly important for tropical watersheds with bimodal precipitation regimes. The new SWAT-Tb variant that we propose here reproduces not only observed streamflow, but also the bimodal seasonal pattern of LAI in a tropical mountain watershed of the Andes. In contrast, standard SWAT is inherently unable to reproduce this bimodality, although it can be calibrated to reproduce streamflow. Differences between models in the representation of LAI seasonality can lead to significantly different results about LULC change impacts on streamflow. SWAT-Tb results show that deforestation impacts on streamflow are more pronounced for seasonal than for annual streamflow, and indicate that forests can play a crucial role in enhancing water availability during dry seasons. The seasonality of streamflow anomalies is switched due to forest-to-pasture conversion, implying that while forest expansion increases water availability in dry seasons, forest conversion into pasture decreases it. Due to its poor representation of LAI seasonality, standard SWAT largely underestimates this role of forest, which can be misleading for decision making about water security and forest conservation.

1 Introduction

Changes in Land Use/Land Cover (LULC henceforth) lead to some of the most concerning anthropogenic alterations of hydrological processes and concomitant environmental and social phenomena (Foley et al., 2005; M. Zhang et al., 2017). In a watershed, the transformation of LULC affects multiple aspects and components of the surface water balance, including soil permeability (Benavides et al., 2018), evapotranspiration (Ponette-González et al., 2014), surface runoff (Roa-García et al., 2011), infiltration (Marín et al., 2019), base flow, water yield (Ochoa-Tocachi et al., 2016), energy partitioning (Mercado-Bettín et al., 2019), and, ultimately, the watershed response via streamflow (Muñoz-Villers & McDonnell, 2013; Ramírez et al., 2017) and regulation capacity (e.g. the amplitude of the streamflow regime) (Ochoa-Tocachi et al., 2016; Peña-Arancibia et al., 2019; J. F. Salazar et al., 2018). Projecting the potential impacts of LULC change on watershed response and regulation is critical for water management decisions in a changing environment (Montanari et al., 2013; J. F. Salazar et al., 2018).

Deforestation is one of the most relevant forms of LULC change, especially in regions like tropical South America with historically high deforestation rates that may be exacerbated by climate change and complex social issues (Zemp et al., 2017; A. Salazar et al., 2018; Duque-Villegas et al., 2019). This is particularly problematic in the tropical Andes, where water and related energy security rely largely on streamflow from mountain watersheds (Viviroli et al., 2007; Sáenz et al., 2014; Angarita et al., 2018; Immerzeel et al., 2020). Major LULC trends in this region include the transformation of Andean forest and paramo vegetation to pastures for cattle raising (García-Leoz et al., 2017), agricultural systems (Clerici et al., 2019), and forest plantations (Bonnesoeur et al., 2019). Field observations show that forest conversion into pasture or crops is associated with changes in the water balance components and related surface properties such as soil permeability, surface runoff, and infiltration (Ramírez et al., 2017; Marín et al., 2019; Suescún et al., 2017). Therefore, understanding the potential impacts of forest loss on streamflow is needed for the assessment of threats to sustainability, especially in mountain watersheds that are becoming increasingly critical for water security in lowland populations (Immerzeel et al., 2020; Viviroli et al., 2020).

The effects of LULC change on watershed response are largely assessed through hydrological models (e.g. M. Zhang et al., 2017; Dos Santos et al., 2018; Peña-Arancibia et al., 2019). Hydrological models are generally able to reproduce observed streamflow (Krysanova et al., 2017). This is a result of, first, models being built upon physical principles, the main of which is mass (water) conservation; and second, of models having numerous parameters that can be tuned to reproduce observations (i.e. model calibration). However, the capability of making reliable projections (e.g. for LULC scenarios) depends on the potential of these models to reproduce the system's behavior for the right reasons (Kirchner, 2006). When the performance of hydrological models is largely, or exclusively, evaluated by comparing simulated and observed streamflow (e.g. Setegn et al., 2010; Villamizar et al., 2019), there is a danger of ignoring unrealistic representations of other important water balance components and related processes.

The Soil and Water Assessment Tool (SWAT) is among the most widely used hydrological models for investigating LULC change impacts on watershed response (Marin et al., 2020; Tan et al., 2020). One of the most critical model components for this task is the vegetation dynamics module (Strauch & Volk, 2013; Alemayehu et al., 2017), since it directly affects the surface water and energy balances (Bonan, 2008). This module includes a plant growth scheme that was originally developed for temperate regions (Neitsch et al., 2011) and, therefore, is not necessarily adequate for tropical regions (Strauch & Volk, 2013; Alemayehu et al., 2017; Hoyos et al., 2019; H. Zhang et al., 2020). This limitation has been partially addressed by using the Leaf Area Index (LAI) to represent vegetation dynamics (Strauch & Volk, 2013; Alemayehu et al., 2017; Ma et al., 2019; Rajib et al., 2020). For instance, Alemayehu et al. (2017) developed a SWAT variant (named SWAT-T) that improves the representation of LAI seasonality in tropical ecosystems, yet still fails to reproduce the bimodal seasonality of LAI that is typical of many of them (Ye et al., 2021) and that is related to the seasonal migration of the ITCZ (Urrea et al., 2019; Knoben et al., 2019). An improved representation of vegetation dynamics is needed to improve the potential of SWAT to produce reliable projections of LULC change impacts (Marin et al., 2020).

The goals of the present study were, first, to improve the representation of tropical vegetation dynamics in SWAT, and then to use the improved model for studying the potential impacts of LULC change on the response of a tropical watershed. More specifically, here we introduce a modification in the plant growth module of SWAT to improve the representation of LAI seasonality, which leads to a new variant that we refer to as SWAT-Tb. Then we compare the performance of SWAT-Tb with other SWAT variants (i.e. standard or default SWAT (Revision 627) and SWAT-T), and show that, in contrast to these other variants, SWAT-Tb produces a realistic representation of not only streamflow but also LAI. Finally, we use SWAT-Tb to study the potential effects of LULC change on streamflow, particularly the expansion of either forest or pasture cover, in a tropical mountain watershed; and show that using the standard SWAT can lead to misleading conclusions.

2 Revision of SWAT Model

The new variant of SWAT, namely SWAT-Tb, introduces a bimodal representation of vegetation dynamics into the SWAT-T model of Alemayehu et al. (2017). SWAT-Tb accounts for the bimodal seasonality of LAI that is typical of many watersheds in tropical (Hoyos et al., 2019; Knoben et al., 2019) and non-tropical (Alhamad et al., 2007; Yang et al., 2019) regions. In the following sections, we provide background on the SWAT model and explain the changes in the new variant.

2.1 Model Description and Limitations

SWAT is a public domain, watershed-scale, process-based, hydrological model (Arnold et al., 1998; Neitsch et al., 2011) that can simulate the response of watersheds (e.g. streamflow) to a variety of forcings, including both climate and LULC change (Gassman et al., 2014; Tan et al., 2020). It is a semi-distributed model wherein a watershed is divided into sub-basins that are further divided into Hydrologic Response Units (HRUs), which are characterized by uniform soil, slope, LULC, and management attributes. Hydrological processes simulated by SWAT include evapotranspiration, surface runoff, percolation, lateral flow, groundwater flow, transmission losses, and ponds (Arnold et al., 2012). The model also includes parameterizations for processes such as plant growth, erosion, nutrients cycling, and pesticides degradation (Neitsch et al., 2011).

The most common formulation for vegetation dynamics in SWAT uses a plant growth module that simulates leaf area development, light interception, and conversion of intercepted light into biomass (Neitsch et al., 2011). This module is based on the Environmental Policy Impact Climate (EPIC) model (Williams et al., 1989) that was developed for temperate regions and is not suitable for all tropical regions (Strauch & Volk, 2013; Alemayehu et al., 2017). A key reason for this is that the EPIC-based module assumes that plant growth, including leaf area development, is mainly controlled by variations in temperature and daylength, which is especially relevant for temperate environments (Mwangi et al., 2016). For instance, this module assumes that plant growth is reduced as daylength approaches that of the shortest day of the year (winter solstice) due to dormancy (Arnold et al., 1998). However, tropical vegetation dynamics can be much less influenced by temperature and daylenght-driven dormancy (Ma et al., 2019), and instead much more controlled by precipitation through soil moisture (X. Zhang et al., 2006). Indeed, in our study watershed, seasonal LAI is more related to precipitation than to temperature (see Section 4.1). This model limitation and its implications for water balance have been highlighted in several studies (Wagner et al., 2011; Strauch & Volk, 2013; Alemayehu et al., 2017; Hoyos et al., 2019; Ma et al., 2019; Rajib et al., 2020; H. Zhang et al., 2020; Marin et al., 2020).

Recognizing this limitation, previous studies have introduced novel representations of vegetation dynamics into SWAT, which have produced satisfactory results for regions like Central Brazil (Strauch & Volk, 2013), Kenya and Tanzania (Alemayehu et al., 2017), southeast China (Ma et al., 2019), north central United States (Rajib et al., 2020), and northern Australia (H. Zhang et al., 2020). For instance, Alemayehu et al. (2017) successfully implemented their new SWAT-T variant in a tropical watershed in Kenya and Tanzania after having modified the plant growth module. Many tropical watersheds, however, do not conform to the unimodal cycle as prescribed in SWAT-T. In fact, Hoyos et al. (2019) showed that although SWAT-T successfully reproduces streamflow in a watershed of the tropical Andes and improves the representation of LAI dynamics as compared to SWAT, it nevertheless fails in reproducing the observed bimodal seasonality of LAI.

2.2 Changes in Plant Growth Module in SWAT-Tb

We built upon SWAT-T's vegetation module to develop SWAT-Tb. This enhanced module has the capability of representing a bimodal LAI annual cycle. SWAT-T uses changes in the Soil Moisture Index (SMI, computed as the ratio between 5-day aggregate precipitation (P) and reference evapotranspiration (ET)) as a proxy for the dry to wet season transition in the tropics, which then triggers a unimodal vegetation growth cycle (Alemayehu et al., 2017). Unlike SWAT-T, SWAT-Tb uses precipitation as a proxy for seasonal variations in LAI. This relation is based also on the assumption that the onset of the wet season triggers plant growth (Liang et al., 2020), and agrees with observations of the annual cycles of precipitation and LAI in the study watershed (see Section 4.1). Using precipitation (as in SWAT-Tb) instead of SMI (as in SWAT-T) is also consistent with the fact that tropical environments are not always water-limited (Gotsch et al., 2016), therefore there is not always a direct relation between plant growth and soil moisture (Alemayehu et al., 2017). In the energy-limited environments that are common in the tropical Andes, precipitation is arguably a better proxy of vegetation dynamics because it relates to both water and energy (e.g. peak LAI comes after peak precipitation as shown in Section 4.1). Seasonal precipitation in the tropical Andes is strongly controlled by the latitudinal migration of the ITCZ (Espinoza et

Table 1. Description of data used in this study.

Data	Description	Source
DEM	Elevation data at a resolution of 1 arc-second (30 meters).	Jarvis et al. (2008)
Land cover	Land cover map for the Grande and Chico rivers watersheds for the year 2015, scale 1:100,000.	CORANTIOQUIA and UNAL (2015)
Soil	Soil map for the the Grande and Chico rivers watersheds, scale 1:50,000.	Machado et al. (2019)
Hydrometeorological	Precipitation, minimum and maximum temperature, relative humidity, evapotranspiration, and streamflow for the period 1990–2016.	EPM[1] and IDEAM[2]
LAI	MCD15A2Hv006 MODIS-LAI product for the period 2003–2016 with a spatial resolution of 0.5 km. Values are 8-days-composites.	Myneni et al. (2015)

[1]EPM: Public Utilities Company of Medellín, [2]IDEAM: Colombian Institute of Hydrology, Meteorology and Environmental Studies.

al., 2020), which affects the surface energy balance, and therefore other vegetation-related variables such as photosynthetic rate, net productivity, and transpiration (Aparecido et al., 2018). The SWAT-Tb executable and the associated changes with file examples (*.sub, *.mgt and plant.dat) can be found in Supplementary Material S1.

3 Materials and Methods

3.1 Study Area

This study focuses on the Chico River (CR) watershed in the tropical Andes of Colombia (Figure 1). The CR watershed is a tributary of the Grande River (GR) watershed, which is strategic for water supply to local rural communities and more than 4 million people living in the Metropolitan Area around Medellín, as well as for hydropower generation (the CR flows into a reservoir, Figure 1d), agriculture, and dairy industry. The CR watershed covers a drainage area of 169 km^2 with altitudes ranging between 2400 and 3260 m.a.s.l. (Figure 1e). Mean annual precipitation is 1820 mm, and mean monthly temperature varies between 12°C and 16°C with an average of 14°C. Precipitation seasonality is characterized by a bimodal regime with two wet seasons: March-April-May (MAM) and September-October-November (SON), and two dry seasons: December-January-February (DJF) and June-July-August (JJA) (Poveda, 2004; García-Leoz et al., 2017). Land use in the watershed is dominated by pastures (54.17% of the area), followed by native forest (29.30%), shrubs (11.42%), and paramo vegetation (4.89%) (Figure 1e). A considerable fraction of native vegetation (e.g. native forest, shrubs, and paramo vegetation) has been converted into agro-pastoral uses in the watershed (Berrouet et al., 2020). The dominant soil type is Andic Dystrudepts, which makes up 62% of the watershed (Figure 1g).

3.2 Input Datasets and Model Parameters

A summarized description of the data used in this study and their sources are presented in Table 1. Elevation data were used for the definition of sub-basins and HRUs. Based on previous studies for tropical Andean regions, the LULC map was reclassified to match the SWAT land use types (Supplementary Table S1; (Tapasco et al., 2015; Hoyos et al., 2019; Villamizar et al., 2019)), and the soil map was parameterized (Machado et al., 2019; Uribe et al., 2018, 2020). Processing of the above data yielded 7 sub-basins and 649 HRUs using the SWAT2012 extension (version 1.9) within QGIS 2.6.1 (Dile et al., 2019) software.

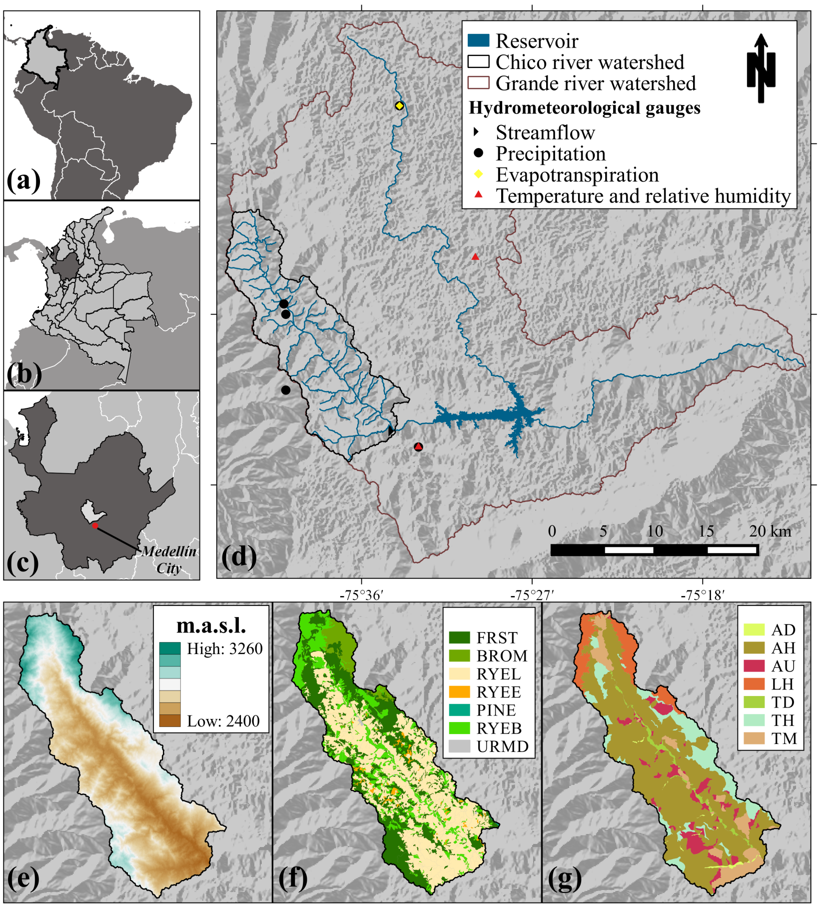

Figure 1. (a-c) General location of the study area (South America, Colombia, and Antioquia, respectively). (d) Grande ("big") and Chico ("small") rivers watersheds including hydrometeorological gauges. (e) Digital Elevation Model (DEM), (f) land cover for the year 2015, and (g) soil types. Land cover and soil types codes are: RYEL: pasture, FRST: native Andean forest, RYEB: shrubs, BROM: paramo vegetation, RYEE: pasture with secondary growth, PINE: planted forest, URMD: urban, AD: Andic Dystrudepts, AH: Andic Humudepts, AU: Andic Udifluvents, LH: Lithic Hapludand, TD: Typic Dystrudepts, TH: Typic Hapludands, and TM: typic melanudands.

Daily hydrometeorological data (precipitation, maximum and minumum temperature, relative humidity, evapotranspiration, and streamflow) from the available gauges (Figure 1d) were provided by the Colombian Institute of Hydrology, Meteorology and Environmental Studies (IDEAM in Spanish) and the Public Utilities Company of Medellín (EPM in Spanish). We used the Priestley-Taylor equation to calculate evapotranspiration as wind data were not available from ground-based gauges, and global datasets (reanalyses) have a limited capacity to represent wind over the complex terrain of the Andes (Posada-Marín et al., 2019). The SWAT's internal WGENX weather generator (Neitsch et al., 2011) was used to estimate daily solar radiation. Observed 8-day composites of LAI were obtained from the MCD15A2H-MODIS product (Myneni et al., 2015) for the 2003–2016 period at 0.5 km spatial resolution. Further details on LAI data processing are given in Section S2 of the Supplementary Material.

3.3 Model Calibration, Validation and Uncertainty Estimation

The SWAT-Tb model is calibrated to simulate, first, monthly LAI, and then monthly streamflow using both manual and automatized techniques. Parameters are initially selected based on a literature review (Arnold et al., 2012; Strauch & Volk, 2013; Abbaspour et al., 2015; Alemayehu et al., 2017; H. Zhang et al., 2020) that includes previous studies for Andean watersheds (Tapasco et al., 2015; Hasan & Wyseure, 2018; Hoyos et al., 2019; Villamizar et al., 2019) (Supplementary Table S3). In order to obtain comparable results, SWAT-T is also calibrated for LAI whereas SWAT is only calibrated for streamflow. Streamflow and LAI calibration was conducted for 2003–2016, while validation was performed for 1993–2002. Three years are added at the beginning of each simulation as a spin-up period to mitigate the influence of uncertain initial conditions, especially for soil moisture. Sensitivity and uncertainty analyses, as well as automatized procedures for calibration and validation are carried out in SWAT-CUP 2019 (version 5.2.1; Abbaspour, 2013) using the Sequential Uncertainty Fitting (SUFI-2) algorithm (Abbaspour et al., 2004).

Calibration of LAI is performed for SWAT-Tb and SWAT-T through manual adjustment of parameters (Supplementary Table S2) while considering land cover types separately. The Breaks for Additive Seasonal and Trend (BFAST) method (Verbesselt et al., 2010) was implemented to exclude noise from the LAI time series. The Pearson correlation coefficient (r), the percent bias (PBIAS), and the Kling–Gupta efficiency (KGE; Gupta et al., 2009) are used to evaluate the agreement between simulated and observed LAI values. Since we want to assess the effect of an inaccurate representation of vegetation dynamics, SWAT is not calibrated for LAI, which is not an unusual practice (e.g. Villamizar et al., 2019; Adhikari et al., 2020). Streamflow calibration is focused on the dominant land cover types —pasture (RYEL) and native Andean forest (FRST) that account for approximately 80% of the watershed (Figure 1f)— and on the upper soil layers that are most directly affected by vegetation change (Tobón et al., 2010; Marín et al., 2019). Parameters for the dominant land cover types are calibrated independently, whereas parameters for all other land cover types are grouped in order to reduce computational cost.

Sensitive parameters are identified with a sensitivity analysis based on 500 simulations. This analysis starts with 33 parameters selected based on previous studies and literature review (Supplementary Table S3), and yields 18 of them as the most sensitive (p-value ≤ 0.05, Supplementary Table S4). We also define an acceptable range of variability for each sensitive parameter. Subsequently, we calibrate monthly streamflow with SUFI-2 using 1000 simulations per iteration (Latin hypercube sampling) for the selected parameter ranges. The calibration goal is to obtain acceptable values for uncertainty statistics (p-value and r-value) and the performance criteria proposed by Moriasi et al. (2007), which include Nash-Sutcliffe Efficiency (NSE) as the objective function and other complementary statistics: percent bias (PBIAS), determination coefficient, and RMSE-observations standard deviation ratio (RSR). We also seek to obtain a reasonable representation of water balance components by considering the following metrics: fraction of total runoff as baseflow, ratio between total evapotranspiration and total precipitation, and ratio between surface runoff and total streamflow. Model outputs for these metrics are compared with observation-based estimates for Andean watersheds (Jaramillo-Robledo, 2003; García-Leoz et al., 2017; Suescún et al., 2017; Bonnesoeur et al., 2019; Marín et al., 2019) (Supplementary Table S4).

3.4 LULC Scenarios

A control (CTL) scenario (i.e. LULC distribution for 2015 (CORANTIOQUIA & UNAL, 2015), Figure 1f) and two extreme LULC scenarios are simulated: full watershed forest loss (100% pasture, PAS) and forest cover (100% forest, FOR). These are not realistic but "baseline"-type scenarios that are used to study the range of potential changes in streamflow due to forest change in the watershed (e.g. Alvarenga et al., 2016; Tian et al., 2017; Li et al., 2019; Peña-Arancibia et al., 2019). These scenarios not only represent changes in the cover (e.g. LAI) but also in some soil properties based on parameterization of land cover types, to obtain a more realistic assessment of forest loss and intensive pasture management impacts on water balance (Tobón et al., 2010; Marín et al., 2019; Peña-Arancibia et al., 2019). Each scenario is simulated for the period 1993–2016 (plus a spin-up period of three years) using the best-fit parameter values from the calibration along with 1000 random combinations within the acceptable ranges. These simulations are performed using the SUFI-2 algorithm (Abbaspour et al., 2004) and their output is used to assess the effects of parameter variability and uncertainty on the results. Differences between scenarios are analyzed using the non-parametric Wilcoxon rank-sum and signed-rank tests (Bauer, 1972). Since everything else is equal, these differences are entirely attributable to LULC change.

3.5 Comparison of SWAT variants

Three variants of the SWAT model that differ in their plant growth module are used: SWAT (default version, Arnold et al., 2012), SWAT-T (Alemayehu et al., 2017), and SWAT-Tb (present study). These variants are compared to evaluate their performance in reproducing the observed dynamics of plant growth, specifically LAI (see Section 4.1). As a proof-of-concept, we also compare SWAT calibrated for streamflow with SWAT-Tb calibrated for both LAI and streamflow.

4 Results

4.1 LAI Calibration

The observed seasonality of precipitation and LAI for all vegetation types in the watershed exhibits a marked bimodal regime (Figure 2). There are two wet seasons in MAM and SON, and two "dry" (less rainy) seasons in DJF and JJA. The SMI follows this same pattern. Relative to precipitation and SMI, LAI exhibits a pattern that can be described as mirrored to precipitation with lower values around the wet seasons and higher values in the dry seasons, which indicates energy-limited ecosystems. This suggests that during the dry seasons plant growth is not as limited by reduced precipitation and moisture (SMI is greater than 1 in all months but January) as it is enhanced by increased radiation resulting from less cloud cover (Aparecido et al., 2018). These results confirm the role of precipitation (and cloudiness) in controlling vegetation seasonality, which according to our results and previous observations appears to be greater than that exerted by temperature. This contrasts the assumptions made in the EPIC model about the dominant role of temperature in plant growth (Williams et al., 1989; Arnold et al., 2012).

Comparison between observed and simulated LAI using SWAT, SWAT-T, and SWAT-Tb for the dominant LULC types shows that SWAT fails to represent LAI seasonality, as evinced by high biases ($53\% < |\mathrm{PBIAS}| < 90\%$) and negative or low correlations ($-0.51 < r < 0.13$). Results for other LULC types are shown in Supplementary Figure S1. A default

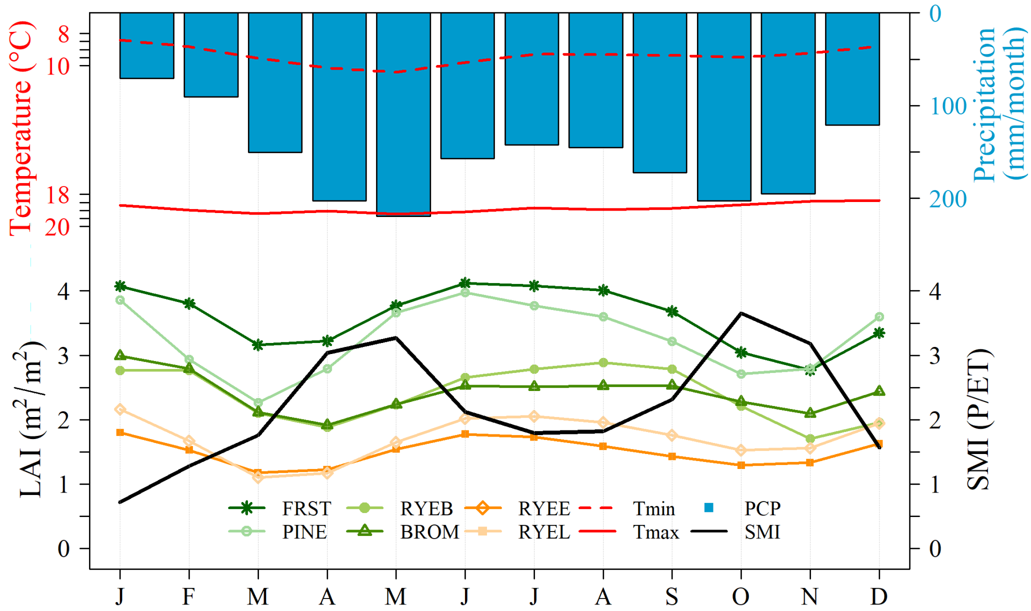

Figure 2. Average seasonality of climate variables (1990–2016; gauging stations) and LAI (2003–2016; BFAST-MODIS; area weighted HRU mean) in the CR watershed. Land cover types as in Figure 1.

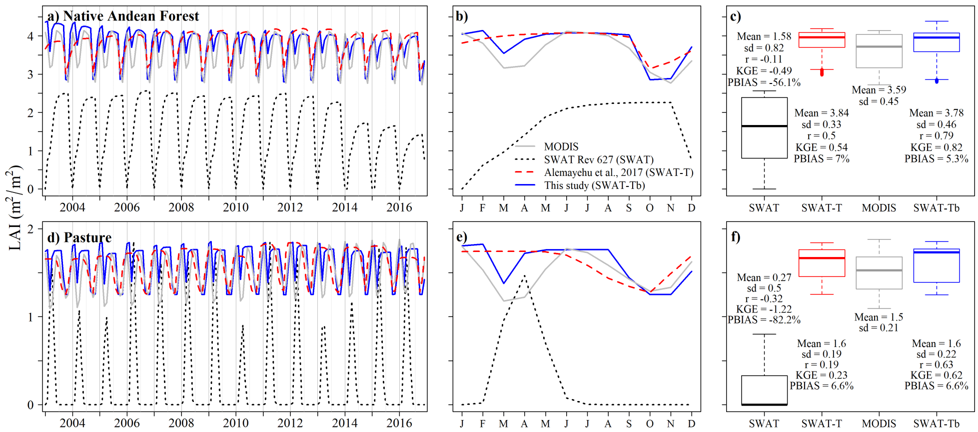

Figure 3. Observed (MODIS) and simulated (SWAT, SWAT-T, and SWAT-Tb) seasonality of LAI in the CR watershed for native Andean forest (top) and pasture (bottom). Time series (a, d), average annual cycle (b, e), and the corresponding box-plots and performance statistics (c, f).

assumption of the SWAT model is that LAI is zero at the beginning of each simulation year, which is unrealistic for tropical vegetation. This assumption is kept for the proof-of-concept, and because it is behind an important limitation of SWAT for tropical watersheds (Strauch & Volk, 2013; Mwangi et al., 2016; Alemayehu et al., 2017; Hoyos et al., 2019; H. Zhang et al., 2020). Regardless of whether this assumption is changed, SWAT does not reproduce LAI bimodality. Calibrated SWAT-T realistically reproduces the range of variability of LAI but fails to represent LAI bimodality because it has a prescribed unimodal regime with a single vegetation growth cycle per year (Alemayehu et al., 2017; Hoyos et al., 2019). Calibrated SWAT-Tb outperforms both SWAT and SWAT-T in reproducing the observed bimodality of LAI, as indicated by the correlation values.

4.2 Streamflow Calibration and Validation

SWAT-Tb is calibrated for streamflow by varying the most sensitive parameters (Supplementary Table S3). The best-fit parameter values and acceptable ranges (i.e. range of parameter values for which simulations are acceptably realistic) are presented in Table 2. Simulated and observed monthly streamflow are shown in Figure 4 for the calibration (2003–2016) and validation (1993–2002) periods. Based on multiple criteria (NSE, RSR, and PBIAS), the model performance can be considered as "very good" and "good" for calibration and validation, respectively (Moriasi et al., 2007). Furthermore, water balance components are realistic as compared to the reference values (Supplementary Table S4).

Likewise, using the best-fit parameter values in Table 2, the performance of standard SWAT in reproducing observed streamflow varies between "very good" (for calibration) and "good" (for validation) (Moriasi et al., 2007, Supplementary Figure S2). This illustrates how standard SWAT can show high performance to reproduce streamflow despite having a low capability to simulate dynamics of LAI (Figure 3 and Supplementary Figure S1).

4.3 Forest versus Pasture Impacts on Streamflow

SWAT-Tb results show that the potential impact of forest cover change on the watershed response is much more pronounced in monthly (Figure 5c) than in annual streamflow (Figure 5f). The results based on annual streamflow would misleadingly indicate that there are small differences between the FOR and PAS scenarios. In contrast, forest change leads to

Table 2. Best-fit values for parameters and their acceptable range for the calibrated SWAT-Tb model.

Parameter[1]	Description	Scaling type[2]	Range min	Range max	Best-fit value
CN2.mgt_RYEL	Runoff curve number for moisture condition II.	r	-0.22	-0.20	-0.20
ESCO.hru_RYEL	Soil evaporation compensation factor.	v	0.35	0.50	0.42
ESCO.hru_FRST	Soil evaporation compensation factor.	v	0.25	0.40	0.27
ALPHA_BF.gw	Baseflow alpha factor (1/days).	v	0.030	0.045	0.030
CN2.mgt_FRST	Runoff curve number for moisture condition II.	r	-0.20	-0.18	-0.19
SOL_K(1).sol_RYEL	Saturated hydraulic conductivity (mm/hr).	r	-0.35	-0.2	-0.23
GWQMN.gw_FRST	Threshold depth of water in the shallow aquifer required for return flow to occur (mm H_2O).	v	1500	2000	1988.25
CH_K2.rte	Effective hydraulic conductivity in main channel alluvium (mm/hr).	v	25	75	52.63
GWQMN.gw_RYEL	Threshold depth of water in the shallow aquifer required for return flow to occur (mm H_2O).	v	2000	2500	2490.25
ESCO.hru_BPRR	Soil evaporation compensation factor.	v	0.15	0.30	0.29
SOL_K(1).sol_FRST	Saturated hydraulic conductivity (mm/hr).	r	-0.20	-0.10	-0.16
SOL_BD(1).sol_BPRR	Moist bulk density (g/cm^3).	r	-0.15	0.0	-0.039
CN2.mgt_BPRR	Runoff curve number for moisture condition II.	r	-0.18	-0.15	-0.17
SOL_AWC(1).sol_FRST	Available water capacity of the soil layer (mm H_2O/mm soil).	r	-0.30	-0.15	-0.25
SOL_BD(1).sol_RYEL	Moist bulk density (g/cm^3).	r	0.15	0.25	0.24
GWQMN.gw_BPRR	Threshold depth of water in the shallow aquifer required for return flow to occur (mm H_2O).	v	1800	2200	1866.20
SOL_K(1).sol_BPRR	Saturated hydraulic conductivity (mm/hr).	r	-0.15	0.0	-0.08
SOL_AWC(1).sol_RYEL	Available water capacity of the soil layer (mm H_2O/mm soil).	r	0.35	0.50	0.37

[1]Numbers (1, 2) refer to the soil layer number. FRST: native Andean forest, RYEL: pasture, and BPRR: paramo vegetation, planted forest, shrubs, and pasture with secondary growth. [2]Scaling type: v (absolute) indicates that the parameter is replaced by the given value, r (relative) indicates that the parameter is multiplied by [1 + (given value)], which preserves spatial variability.

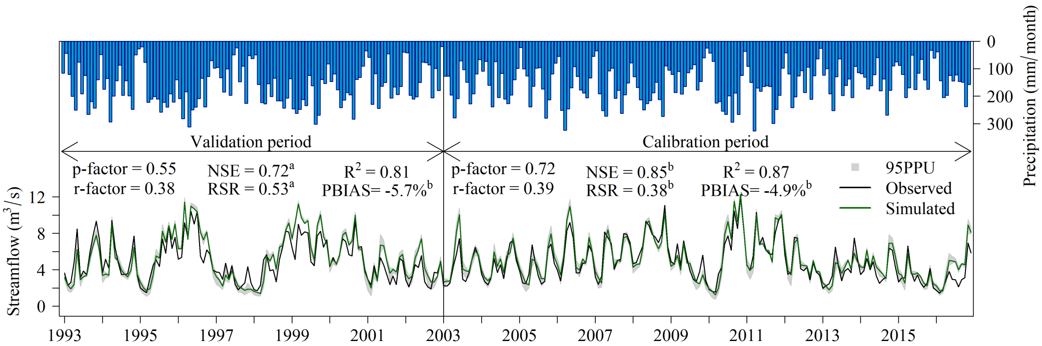

Figure 4. Calibration (2003–2016) and validation (1993–2002) of SWAT-Tb for monthly streamflow. Vertical bars show monthly rainfall from SWAT output, calculated from records in climate stations. NSE: Nash-Sutcliffe coefficient, PBIAS: percent bias, R^2: coefficient of determination, and RSR: RMSE-observations standard deviation ratio. 95PPU: the 95% prediction uncertainty. Model performances based on the criteria of Moriasi et al. (2007): ^{a} Good ($0.65<\text{NSE}\leq 0.75$, $0.50<\text{RSR}\leq 0.60$, $\pm 10\%<\text{BIAS}< \pm 15\%$) and ^{b} Very Good ($0.75<\text{NSE}\leq 1.00$, $0.00<\text{RSR}\leq 0.50$, $\text{BIAS}\leq \pm 10\%$).

significant differences in monthly streamflow seasonality, which are particularly pronounced during the dry seasons (DJF and JJA). The occurrence of 100% forest cover in the watershed leads to increased streamflow during the dry seasons (e.g. average streamflow in January is about 10% greater in the FOR than in the CTL scenario), whereas its absence causes a streamflow reduction (e.g. average streamflow in January is about 6% lower in the PAS than in the CTL scenario). During the wet seasons, the most significant difference is found in April when streamflow is reduced in the FOR scenario, while it is increased in the PAS scenario. Differences between scenarios are smaller in the SON wet season. These results remain valid when considering 1000 combinations of parameters values within the acceptable ranges (Supplementary Figure S3).

Differences between scenarios seem small when looking at box-plots for the annual cycle (Figure 5b) and annual average (Figure 5e). This is because these box-plots do not show the year-to-year variability of monthly streamflow. Figures 5c and 5f clarify this by showing the distribution (box-plots) of monthly differences computed as the difference of streamflow between scenarios for the same month and year. This is important to guarantee that the comparison is done between LULC scenarios under the same climate forcing (precipitation and temperature). For instance, PAS scenario streamflow under La Niña conditions (above-normal precipitation) is not comparable to FOR scenario streamflow under El Niño conditions (below-normal precipitation).

Despite their comparable ability to reproduce observed streamflow, SWAT and SWAT-Tb results do not support the same conclusions. For instance, streamflow increase in the FOR scenario during the dry seasons is largely underestimated (in DJF) or even reversed (in July and August) (Figure 5c) in SWAT output. The median percent increase of streamflow from SWAT can be less than half the corresponding increase in SWAT-Tb (e.g. $\sim 4\%$ versus $\sim 10\%$ in January). Further, SWAT results indicate that the median annual streamflow would barely change due to extensive modification of LULC in the FOR and PAS scenarios (Figure 5d). In contrast, SWAT-Tb output show a greater change in the median annual streamflow. The statistical significance of this change will be discussed below.

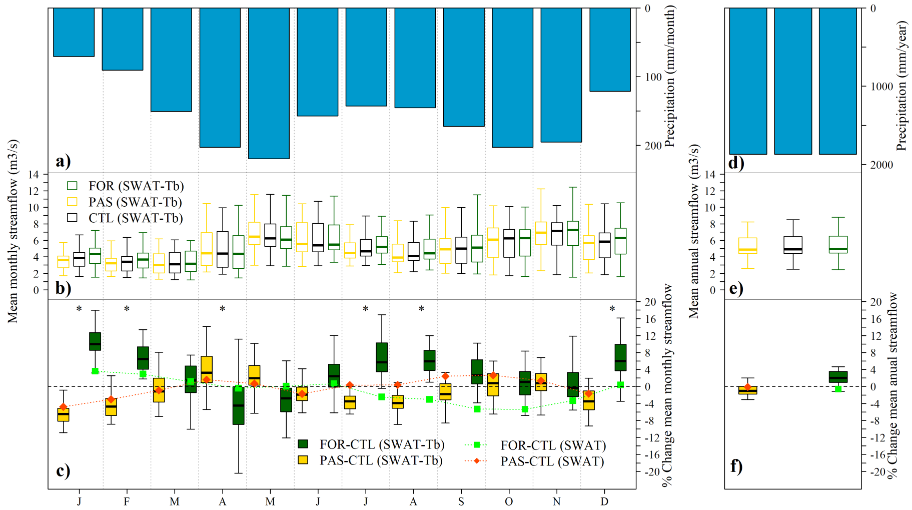

Figure 5. Comparison of monthly (left) and annual (right) streamflow between scenarios and models. Input precipitation (blue bars) is the same for all scenarios and models (a,d). Average annual cycle (b) and annual streamflow (e) in all scenarios for 1993–2016. Percent differences between monthly (c) and annual (f) streamflow in the control (CTL) and LULC (FOR and PAS) scenarios for 1993–2016 as simulated by SWAT-Tb and SWAT using best fit parameters. Positive (negative) values indicate that streamflow is increased (decreased) in the LULC change scenario. Boxes (dark green and yellow) show variability of monthly differences in SWAT-Tb output, whereas lines with dots (light green and orange) show the corresponding median from SWAT output. Asterisks identify months for which the difference between medians in the FOR and PAS scenarios is statistically significant (n=24, $p < 0.05$) for SWAT-Tb output.

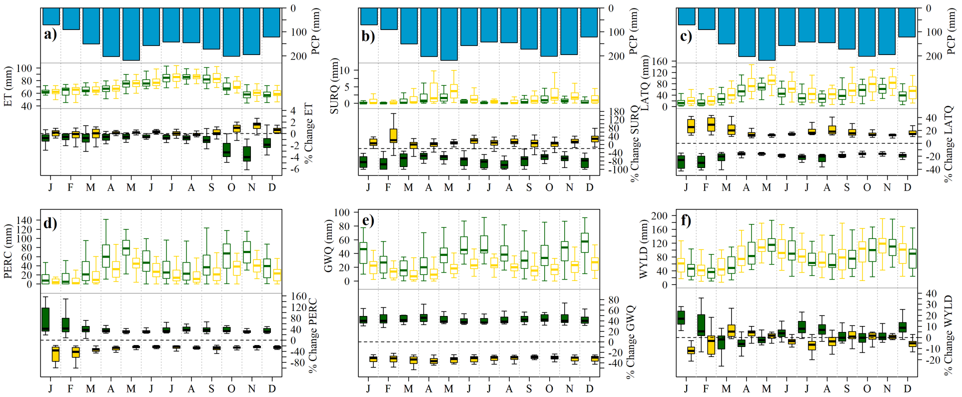

Figure 6. Annual cycle and percent differences between monthly (a) actual evapotranspiration (ET), (b) surface runoff (SURQ), (c) lateral flow (LATQ), (d) percolation (PERC), (e) groundwater contribution to streamflow (GWQ), and (f) water yield (WYLD) in the control (CTL) and LULC (FOR and PAS) scenarios for 1993–2016 as simulated by SWAT-Tb at the watershed scale. Variables are HRU area-weighted means for each month. Positive (negative) values indicate that the variable is increased (decreased) in the LULC change scenario. Vertical bars show mean monthly precipitation (PCP).

4.4 Water Balance Components

Differences in streamflow between scenarios are caused by differences in the watershed's water balance components (Figure 6). The largest differences between the CTL and LULC scenarios are found for surface runoff (Figure 6b), lateral flow (Figure 6c), percolation (Figure 6d), and groundwater contribution (i.e. baseflow) to streamflow (Figure 6e). The sum of these differences leads to differences in water yield (Figure 6f). By comparison, differences in evapotranspiration are much less pronounced (Figure 6a; note that their magnitudes never exceed 6%). All these differences consider the year-to-year variability as explained previously for Figure 5.

In our simulations, differences between output from SWAT-Tb and SWAT are entirely caused by differences in the simulated LAI values (Figure 7a). The resulting differences in water balance components are more pronounced for the PAS than for the FOR scenario (Figure 7b–g). As compared to SWAT-Tb, in the PAS scenario SWAT overestimates water yield throughout the year (Figure 7g), with larger values during JJA and SON, i.e. during the second dry and wet seasons of the year in the actual bimodal regime. This overestimation in JJA–SON results from greater production of surface runoff (Figure 7c), lateral flow (Figure 7d), and base flow (Figure 7f), as well as from reduced evapotranspiration (Figure 7b). In DJF–MAM, there are mixed patterns in the water balance components that lead to a smaller overestimation of water yield. In the FOR scenario, SWAT underestimates LAI throughout the year, mostly in DJF, which leads to mixed results in water balance components. In both scenarios, differences of surface runoff between models (Figure 7c) are minimal ($< \pm$ 0.5 mm), hence the effects on streamflow result mainly from variations in evapotranspiration and groundwater flows (i.e. lateral flow, percolation, and base flow).

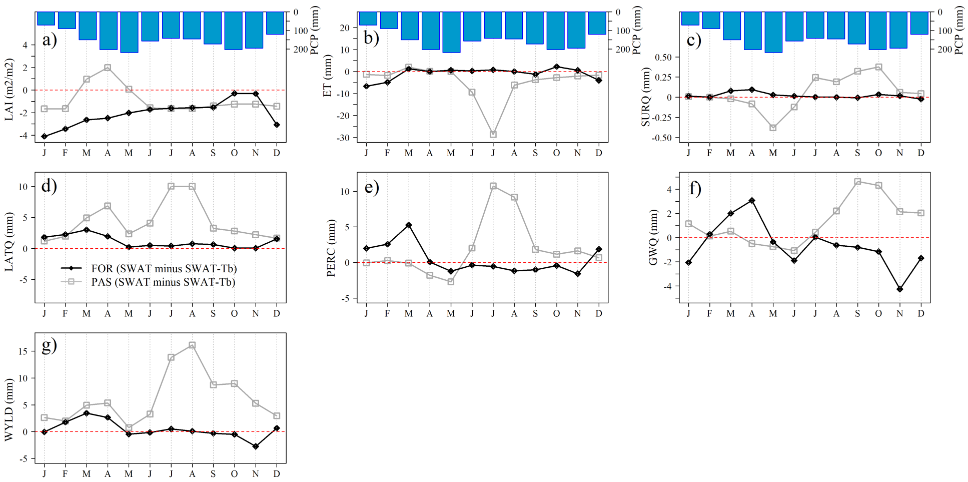

Figure 7. Differences between SWAT and SWAT-Tb in the monthly median of (a) Leaf Area Index (LAI), (b) total biomass (BIOM, i.e. above-ground and roots at the end of the period reported as dry weight), (c) actual evapotranspiration (ET), (d) surface runoff (SURQ), (e) lateral flow (LATQ), (f) percolation (PERC), (g) groundwater contribution (GWQ), and (h) water yield (WYLD) for each LULC scenario (PAS and FOR) at the watershed scale (area-weighted HRU mean for each month).

5 Discussion

5.1 Advantages of SWAT-Tb over SWAT

There is no noticeable difference between SWAT-Tb and SWAT in representing monthly streamflow (Figures 5b and S2). However, there are visible differences in their capability to reproduce vegetation dynamics through LAI (Figure 3), as well as in their results regarding the potential impact of forest conversion on streamflow (Figure 5c) and the underlying changes in the water balance components (Figure 7).

Our proof-of-concept illustrates how SWAT can be calibrated to realistically simulate streamflow despite being intrinsically unable to reproduce the observed dynamics of LAI, which has multiple effects on the water balance components including evapotranspiration, canopy interception, and surface runoff (Neitsch et al., 2011; Strauch & Volk, 2013; Alemayehu et al., 2017). Hence, there is a danger of getting the right results (e.g. the model reproduces observed streamflow) for the wrong reasons (Kirchner, 2006), which strongly limits the capability of models (i.e. SWAT in the present case) to produce reliable results for informing decisions.

We argue that SWAT results (Figures 5 and 7), and perhaps also the results of studies using the approach of calibrating and validating SWAT for streamflow but not for LAI (e.g. Villamizar et al., 2019; Adhikari et al., 2020), may be misleading about the impacts of tropical forest change on streamflow. In contrast, SWAT-Tb provides better insight by reproducing not only the observed streamflow but also the bimodal dynamics of LAI that are typical of many tropical watersheds. This is particularly important for assessing water balance components that affect water security in the tropical Andes threatened by undergoing deforestation (A. Salazar et al., 2018; Viviroli et al., 2020).

5.2 Forest Impact on the Watershed's Regulation Capacity and Water Availability

Results of previous studies about forest change impacts on streamflow are diverse (M. Zhang et al., 2017; Ochoa-Tocachi et al., 2016; Jones et al., 2020), which suggests that conclusions about this are hardly generalizable. However, a number of previous studies have concluded that increased forest cover in a watershed leads to decreased annual streamflow, mainly as a consequence of increased evapotranspiration (Ellison et al., 2012; Muñoz-Villers & McDonnell, 2013; Ogden et al., 2013; M. Zhang et al., 2017). In our results, differences in annual streamflow between scenarios are not statistically significant ($p > 0.05$; Figure 5f and Supplementary Figure S3f), which does not necessarily imply that these differences are negligible or physically meaningless (Amrhein et al., 2019). Given this, and in addition to the significant differences in the annual cycle, our results indicate that annual streamflow is almost always greater in the FOR than in the CTL and PAS scenarios, which is opposite to the aforementioned conclusion.

There are statistically significant differences in monthly streamflow between scenarios ($p < 0.05$; Figure 5c and Supplementary Figure S3c), particularly in dry seasons (DJF and JJA). This is relevant from the perspective of regulation, defined here as the capacity of watersheds to reduce streamflow variability and attenuating extreme streamflows (Ochoa-Tocachi et al., 2016; J. F. Salazar et al., 2018; Rodríguez et al., 2018). This regulation implies a contrasting capacity of watersheds to increase low streamflows while reducing floods (J. F. Salazar et al., 2018; Rodríguez et al., 2018). The CR watershed's regulation capacity is increased in the FOR scenario, as revealed by higher streamflow during the dry season while little change during the wet season, relative to the CTL scenario.

Increased forest cover leads to reduced direct runoff and lateral flow, as well as to increased percolation and groundwater contribution to streamflow (i.e. base flow), as compared to the effect of increased pasture cover (Figure 6), which is consistent with field observations in the region of the CR watershed by García-Leoz et al. (2017); Suescún et al. (2017). Although these effects of forest change are the same throughout the year (Figure 6), their impact on streamflow is not the same because it depends on the relative contribution of each water balance component to streamflow. In dry seasons, streamflow depends more on base flow than on direct runoff and lateral flow. In contrast, during wet seasons precipitation may contribute more to streamflow via direct runoff and lateral flow than base flow. As a result, the impacts on streamflow of reduced direct runoff and lateral flow, and increased percolation and base flow, vary across seasons. The increased presence of forest can increase low streamflow during dry seasons mainly through increased base flow, while it can reduce streamflow during the wet season mainly through reduced direct runoff and lateral flow.

These results are consistent with some theoretical hypothesis and previous observational studies. The infiltration trade-off hypothesis for tropical environments (Bruijnzeel, 1989, 2004) proposes that reduced forest cover in a watershed can lead to reduced low streamflow in dry seasons as a result of reductions in infiltration and water storage in soils during wet seasons, which are not compensated by water gains due to reduced evapotranspiration. The forest reservoir hypothesis (J. F. Salazar et al., 2018) proposes that tropical forests enhance the capacity of watersheds to regulate streamflow, mainly through their role in mediating land-atmosphere interactions. Ellison et al. (2012) divide the forest water debate into two schools of thought: the "demand-side" and the "supply-side" schools. While the former sees trees and forests as consumers of available water and competitors for other downstream water uses, the latter supports the beneficial impact of forest cover on the hydrological cycle, emphasizing that increasing forest cover raises water yield. Our results lend support to the "supply-side" perspective.

Observational and modeling studies have shown that forest conversion into pasture or croplands in tropical watersheds can result in decreased low streamflows and increased floods

(Roa-García et al., 2011; Ogden et al., 2013; Ochoa-Tocachi et al., 2016; Ramírez et al., 2017; Krishnaswamy et al., 2018; Peña-Arancibia et al., 2019; López-Ramírez et al., 2020). Our results indicate that forest cover gain (i.e. FOR scenario) leads to increased infiltration and groundwater recharge (Figures 6c-e) and little changes in evapotranspiration (Figures 6a). Field observations in the region of the CR watershed have indicated that the difference between evapotranspiration of native Andean forest (FRST) and pasture (RYEL) is small (García-Leoz et al., 2017), as it is in our results.

6 Conclusions

Bimodal seasonal patterns of vegetation dynamics are common to many watersheds, especially (although not exclusively) in tropical regions under the influence of the ITCZ. The new SWAT-Tb variant reproduces not only observed streamflow, but also the bimodal seasonal pattern of LAI in a tropical mountain watershed. In contrast, standard SWAT is inherently unable to reproduce this bimodality in vegetation dynamics, although it can be calibrated to reproduce streamflow. These variations in the representation of LAI seasonality can lead to significantly different results when assessing LULC change impacts on streamflow.

Regarding the effect of forest change on streamflow, our results show that impacts can be much more pronounced for seasonal than for annual streamflow, and indicate that forests can play a crucial role in enhancing water availability during dry seasons. We found that the seasonality of streamflow anomalies is largely switched due to forest-to-pasture conversion, implying that while forest expansion increases water availability in dry seasons, deforestation (e.g. forest conversion into pasture) can strongly decrease it. Due to its poor representation of LAI seasonality, standard SWAT largely underestimates this role of forest, which can be misleading for decision making about water security and forest conservation.

Data availability

The SWAT-Tb executable and code will be available through SWATshare (`https://mygeohub.org/groups/water-hub/swatshare_landing`), which is a cyberinfrastructure for sharing, simulation, and visualization of SWAT models. For review purposes, the data are available online at `https://bit.ly/2XT8uxs`. After publication, we may change the link to keep the files permanently available in SWATshare. Emails requesting necessary technical support can be directed to the corresponding author. The data used in this study are publicly available. Sources to access these data, including any other information to replicate the results, are provided in the references, tables, and supporting information. Also, they are accessible through links provided below: Digital Elevation Model was from `http://srtm.csi.cgiar.org/`. MODIS-LAI data was obtained from `https://lpdaac.usgs.gov/products/mcd15a2hv006/`. IDEAM from `http://dhime.ideam.gov.co/atencionciudadano/`. Land cover and soil types maps is available through CORANTIOQUIA and UNAL (2015) and Machado et al. (2019), respectively.

Acknowledgments

This work was funded by the Universidad de Antioquia through the Estudiante Instructor Program for graduate studies and Committee for Research Development. JFS and JCV were funded by the Colombian Ministry of Science, Technology and Innovation (MINCIENCIAS) through program "Sostenibilidad de sistemas ecológicos y sociales en la cuenca Magdalena-Cauca bajo escenarios de cambio climático y pérdida de bosques" (code 1115-852-70719) with funds from "Patrimonio Autónomo Fondo Nacional de Financiamiento para la Ciencia, la Tecnología y la Innovación, Fondo Francisco José de Caldas". JCV was supported by the project "Trayectorias de sistemas socio-ecológicos y sus determinantes en cuencas estratégicas en un contexto de cambio ambiental. Código 110180863961, Convocatoria 808-2018 Proyectos de ciencia, tecnología e innovación y su contribución a los retos de país-Colciencias". NH was partially supported by the Fulbright Visiting Scholar Porgram from the Fulbright Commission in Colombia while on research leave from Universidad del Norte, and by The Canadian Queen Elizabeth II Diamond Jubilee Scholarships (QES), a partnership among Universities in Canada, the Rideau Hall Foundation (RHF), Community Foundations of Canada (CFC). The QES-AS is made possible with financial support from IDRC and SSHRC. The authors are grateful to Natalia Uribe and Jenny Machado for their support with setting up SWAT.

References

Abbaspour, K. C. (2013). SWAT-CUP 2012. *SWAT Calibration and Uncertainty Program—A User Manual*.

Abbaspour, K. C., Johnson, C., & Van Genuchten, M. T. (2004). Estimating uncertain flow and transport parameters using a sequential uncertainty fitting procedure. *Vadose Zone Journal*, *3*(4), 1340–1352.

Abbaspour, K. C., Rouholahnejad, E., Vaghefi, S., Srinivasan, R., Yang, H., & Kløve, B. (2015). A continental-scale hydrology and water quality model for Europe: Calibration and uncertainty of a high-resolution large-scale SWAT model. *Journal of Hydrology*, *524*, 733–752.

Adhikari, R. K., Mohanasundaram, S., & Shrestha, S. (2020). Impacts of land-use changes on the groundwater recharge in the Ho Chi Minh city, Vietnam. *Environmental Research*, 109440.

Alemayehu, T., Griensven, A. v., Woldegiorgis, B. T., & Bauwens, W. (2017). An improved SWAT vegetation growth module and its evaluation for four tropical ecosystems. *Hydrology and Earth System Sciences*, *21*(9), 4449–4467.

Alhamad, M., Stuth, J., & Vannucci, M. (2007). Biophysical modelling and NDVI time series to project near-term forage supply: spectral analysis aided by wavelet denoising and ARIMA modelling. *International Journal of Remote Sensing*, *28*(11), 2513–2548.

Alvarenga, L., De Mello, C., Colombo, A., Cuartas, L., & Bowling, L. (2016). Assessment of land cover change on the hydrology of a Brazilian headwater watershed using the Distributed Hydrology-Soil-Vegetation Model. *Catena*, *143*, 7–17.

Amrhein, V., Greenland, S., & McShane, B. (2019). *Scientists rise up against statistical significance.* Nature Publishing Group.

Angarita, H., Wickel, A. J., Sieber, J., Chavarro, J., Maldonado-Ocampo, J. A., Herrera-R, G. A., . . . Purkey, D. (2018). Basin-scale impacts of hydropower development on the Mompós Depression wetlands, Colombia. *Hydrology and Earth System Sciences*, *22*(5), 2839.

Aparecido, L. M. T., Teodoro, G. S., Mosquera, G., Brum, M., Barros, F. d. V., Pompeu, P. V., . . . others (2018). Ecohydrological drivers of Neotropical vegetation in montane ecosystems. *Ecohydrology*, *11*(3), e1932.

Arnold, J., Moriasi, D. N., Gassman, P. W., Abbaspour, K. C., White, M. J., Srinivasan, R., . . . others (2012). Swat: Model use, calibration, and validation. *Transactions of the ASABE*, *55*(4), 1491–1508.

Arnold, J., Srinivasan, R., Muttiah, R. S., & Williams, J. R. (1998). Large area hydrologic modeling and assessment part I: model development. *JAWRA Journal of the American Water Resources Association*, *34*(1), 73–89.

Bauer, D. F. (1972). Constructing confidence sets using rank statistics. *Journal of the American Statistical Association*, *67*(339), 687–690.

Benavides, I., Solarte, M., Pabón, V., Ordoñez, A., Beltrán, E., Rosero, S., & Torres, C. (2018). The variation of infiltration rates and physical-chemical soil properties across a land cover and land use gradient in a Paramo of southwestern Colombia. *Journal of Soil and Water Conservation*, *73*(4), 400–410.

Berrouet, L., Villegas-Palacio, C., & Botero, V. (2020). Vulnerability of Rural Communities to Change in an Ecosystem Service Provision: Surface water supply. A Case Study in the Northern Andes, Colombia. *Land Use Policy*, *97*, 104737.

Bonan, G. B. (2008). Forests and climate change: forcings, feedbacks, and the climate benefits of forests. *science*, *320*(5882), 1444–1449.

Bonnesoeur, V., Locatelli, B., Guariguata, M. R., Ochoa-Tocachi, B. F., Vanacker, V., Mao, Z., ... Mathez-Stiefel, S.-L. (2019). Impacts of forests and forestation on hydrological services in the Andes: A systematic review. *Forest Ecology and Management*, *433*, 569–584.

Bruijnzeel, L. (1989). forestation and dry season flow in the tropics: A closer look. *Journal of Tropical Forest Science*, 229–243.

Bruijnzeel, L. (2004). Hydrological functions of tropical forests: not seeing the soil for the trees? *Agriculture, ecosystems & environment*, *104*(1), 185–228.

Clerici, N., Cote-Navarro, F., Escobedo, F. J., Rubiano, K., & Villegas, J. C. (2019). Spatio-temporal and cumulative effects of land use-land cover and climate change on two ecosystem services in the Colombian Andes. *Science of The Total Environment*, *685*, 1181–1192.

CORANTIOQUIA, & UNAL. (2015). *Actualización y ajuste plan de ordenación y manejo de la cuenca de los ríos grande y chico. municipios de belmira, san pedro de los milagros, entrerríos, santa rosa de osos, donmatías y yarumal. (no. convenio interadministrativo no. 967 de 2013)* (Tech. Rep.). Medellín, Antioquia: Corporación Autónoma Regional del Centro de Antioquia y Universidad Nacional de Colombia Sede Medellín.

Dile, Y., Srinivasan, R., & George, C. (2019). QGIS Interface for SWAT (QSWAT), version 1.9. *Texas AM University*.

Dos Santos, V., Laurent, F., Abe, C., & Messner, F. (2018). Hydrologic Response to Land Use Change in a Large Basin in Eastern Amazon. *Water*, *10*(4), 429.

Duque-Villegas, M., Salazar, J. F., & Rendón, A. M. (2019). Tipping the ENSO into a permanent El Niño can trigger state transitions in global terrestrial ecosystems. *Earth System Dynamics*, *10*(4).

Ellison, D., N. Futter, M., & Bishop, K. (2012). On the forest cover–water yield debate: from demand-to supply-side thinking. *Global Change Biology*, *18*(3), 806–820.

Espinoza, J. C., Garreaud, R., Poveda, G., Arias, P. A., Molina-Carpio, J., Masiokas, M., ... Scaff, L. (2020). Hydroclimate of the Andes Part I: Main climatic features. *Frontiers in Earth Science*, *8*, 64.

Foley, J. A., DeFries, R., Asner, G. P., Barford, C., Bonan, G., Carpenter, S. R., ... others (2005). Global consequences of land use. *science*, *309*(5734), 570–574.

García-Leoz, V., Villegas, J. C., Suescún, D., Flórez, C. P., Merino-Martín, L., Betancur, T., & León, J. D. (2017). Land cover effects on water balance partitioning in the Colombian Andes: improved water availability in early stages of natural vegetation recovery. *Regional Environmental Change*, 1–13.

Gassman, P. W., Sadeghi, A. M., & Srinivasan, R. (2014). Applications of the SWAT model special section: overview and insights. *Journal of Environmental Quality*, *43*(1), 1–8.

Gotsch, S. G., Asbjornsen, H., & Goldsmith, G. R. (2016). Plant carbon and water fluxes in tropical montane cloud forests. *Journal of Tropical Ecology*, *32*(5), 404–420.

Gupta, H. V., Kling, H., Yilmaz, K. K., & Martinez, G. F. (2009). Decomposition of the mean squared error and NSE performance criteria: Implications for improving hydrological modelling. *Journal of hydrology*, *377*(1-2), 80–91.

Hasan, M. M., & Wyseure, G. (2018). Impact of climate change on hydropower generation in Rio Jubones Basin, Ecuador. *Water Science and Engineering*, *11*(2), 157–166.

Hoyos, N., Correa-Metrio, A., Jepsen, S. M., Wemple, B., Valencia, S., Marsik, M., ... Velez, M. I. (2019). Modeling Streamflow Response to Persistent Drought in a Coastal Tropical Mountainous Watershed, Sierra Nevada De Santa Marta, Colombia. *Water*, *11*(1), 94.

Immerzeel, W. W., Lutz, A., Andrade, M., Bahl, A., Biemans, H., Bolch, T., ... others (2020). Importance and vulnerability of the world's water towers. *Nature*, *577*(7790), 364–369.

Jaramillo-Robledo, A. (2003). La lluvia y el transporte de nutrimentos dentro de ecosistemas de bosque y cafetales. *Cenicafé*, *54*(2), 134–144.
Jarvis, A., Reuter, H. I., Nelson, A., Guevara, E., et al. (2008). Hole-filled SRTM for the globe Version 4. *available from the CGIAR-CSI SRTM 90m Database (http://srtm. csi. cgiar. org)*, *15*, 25–54.
Jones, J. A., Wei, X., Archer, E., Bishop, K., Blanco, J. A., Ellison, D., ... Creed, I. F. (2020). Forest-water interactions under global change. In *Forest-Water Interactions* (pp. 589–624). Springer.
Kirchner, J. W. (2006). Getting the right answers for the right reasons: Linking measurements, analyses, and models to advance the science of hydrology. *Water Resources Research*, *42*(3).
Knoben, W. J., Woods, R. A., & Freer, J. E. (2019). Global bimodal precipitation seasonality: A systematic overview. *International Journal of Climatology*, *39*(1), 558–567.
Krishnaswamy, J., Kelkar, N., & Birkel, C. (2018). Positive and neutral effects of forest cover on dry-season stream flow in Costa Rica identified from Bayesian regression models with informative prior distributions. *Hydrological Processes*, *32*(24), 3604–3614.
Krysanova, V., Vetter, T., Eisner, S., Huang, S., Pechlivanidis, I., Strauch, M., ... others (2017). Intercomparison of regional-scale hydrological models and climate change impacts projected for 12 large river basins worldwide—a synthesis. *Environmental Research Letters*, *12*(10), 105002.
Li, F., Zhang, G., Li, H., & Lu, W. (2019). Land Use Change Impacts on Hydrology in the Nenjiang River Basin, Northeast China. *Forests*, *10*(6), 476.
Liang, B., Chen, X., Lang, W., Liu, G., Malhi, Y., & Rifai, S. (2020). Examining land surface phenology in the tropical moist forest eco-zone of South America. *International Journal of Biometeorology*, 1–12.
López-Ramírez, S. M., Sáenz, L., Mayer, A., Muñoz-Villers, L. E., Asbjornsen, H., Berry, Z. C., ... Aguilar, L. R. G. (2020). Land use change effects on catchment streamflow response in a humid tropical montane cloud forest region, central veracruz, mexico. *Hydrological Processes*.
Ma, T., Duan, Z., Li, R., & Song, X. (2019). Enhancing SWAT with remotely sensed LAI for improved modelling of ecohydrological process in subtropics. *Journal of hydrology*, *570*, 802–815.
Machado, J., Villegas-Palacio, C., Loaiza, J. C., & Castañeda, D. A. (2019). Soil natural capital vulnerability to environmental change. A regional scale approach for tropical soils in the Colombian Andes. *Ecological indicators*, *96*, 116–126.
Marín, F., Dahik, C. Q., Mosquera, G. M., Feyen, J., Cisneros, P., & Crespo, P. (2019). Changes in soil hydro-physical properties and SOM due to Pine afforestation and grazing in Andean environments cannot be generalized. *Forests*, *10*(1), 17.
Marin, M., Clinciu, I., Tudose, N. C., Ungurean, C., Adorjani, A., Mihalache, A. L., ... Cacovean, H. (2020). Assessing the vulnerability of water resources in the context of climate changes in a small forested watershed using SWAT: A review. *Environmental Research*, 109330.
Mercado-Bettín, D., Salazar, J. F., & Villegas, J. C. (2019). Long-term water balance partitioning explained by physical and ecological characteristics in world river basins. *Ecohydrology*, *12*(3), e2072.
Montanari, A., Young, G., Savenije, H., Hughes, D., Wagener, T., Ren, L., ... Belyaev, V. (2013). "Panta Rhei—everything flows": change in hydrology and society—the IAHS scientific decade 2013–2022. *Hydrological Sciences Journal*, *58*(6), 1256–1275.
Moriasi, D. N., Arnold, J., Van Liew, M. W., Bingner, R. L., Harmel, R. D., & Veith, T. L. (2007). Model evaluation guidelines for systematic quantification of accuracy in watershed simulations. *Transactions of the ASABE*, *50*(3), 885–900.
Muñoz-Villers, L., & McDonnell, J. (2013). Land use change effects on runoff generation in a humid tropical montane cloud forest region. *Hydrology and Earth System Sciences*, *17*(9), 3543.
Mwangi, H. M., Julich, S., Patil, S. D., McDonald, M. A., & Feger, K.-H. (2016). Mod-

elling the impact of agroforestry on hydrology of Mara River Basin in East Africa. *Hydrological Processes*, *30*(18), 3139–3155.

Myneni, R., Knyazikhin, Y., & Park, T. (2015). *MCD15A2H MODIS/Terra+ Aqua Leaf Area Index/FPAR 8-day L4 Global 500 m SIN Grid V006, NASA EOSDIS Land Processes DAAC.*

Neitsch, S. L., Arnold, J., Kiniry, J. R., & Williams, J. R. (2011). *Soil and water assessment tool theoretical documentation version 2009* (Tech. Rep.). College Station, Texas: Texas Water Resources Institute.

Ochoa-Tocachi, B. F., Buytaert, W., De Bievre, B., Célleri, R., Crespo, P., Villacís, M., ... others (2016). Impacts of land use on the hydrological response of tropical Andean catchments. *Hydrological Processes*, *30*(22), 4074–4089.

Ogden, F. L., Crouch, T. D., Stallard, R. F., & Hall, J. S. (2013). Effect of land cover and use on dry season river runoff, runoff efficiency, and peak storm runoff in the seasonal tropics of central panama. *Water Resources Research*, *49*(12), 8443–8462.

Peña-Arancibia, J. L., Bruijnzeel, L. A., Mulligan, M., & van Dijk, A. I. (2019). Forests as 'sponges' and 'pumps': Assessing the impact of deforestation on dry-season flows across the tropics. *Journal of Hydrology*, *574*, 946–963.

Ponette-González, A. G., Marín-Spiotta, E., Brauman, K. A., Farley, K. A., Weathers, K. C., & Young, K. R. (2014). Hydrologic connectivity in the high-elevation tropics: Heterogeneous responses to land change. *BioScience*, *64*(2), 92–104.

Posada-Marín, J. A., Rendón, A. M., Salazar, J. F., Mejía, J. F., & Villegas, J. C. (2019). WRF downscaling improves ERA-Interim representation of precipitation around a tropical Andean valley during El Niño: implications for GCM-scale simulation of precipitation over complex terrain. *Climate Dynamics*, *52*(5-6), 3609–3629.

Poveda, G. (2004). La hidroclimatología de Colombia: una síntesis desde la escala inter-decadal hasta la escala diurna. *Revista de la Academia Colombiana de Ciencias exactas, físicas y naturales*, *28*(107), 201–222.

Rajib, A., Kim, I. L., Golden, H. E., Lane, C. R., Kumar, S. V., Yu, Z., & Jeyalakshmi, S. (2020). Watershed Modeling with Remotely Sensed Big Data: MODIS Leaf Area Index Improves Hydrology and Water Quality Predictions. *Remote Sensing*, *12*(13), 2148.

Ramírez, B. H., Teuling, A. J., Ganzeveld, L., Hegger, Z., & Leemans, R. (2017). Tropical Montane Cloud Forests: Hydrometeorological variability in three neighbouring catchments with different forest cover. *Journal of hydrology*, *552*, 151–167.

Roa-García, M., Brown, S., Schreier, H., & Lavkulich, L. (2011). The role of land use and soils in regulating water flow in small headwater catchments of the Andes. *Water Resources Research*, *47*(5).

Rodríguez, E., Salazar, J. F., Villegas, J. C., & Mercado-Bettín, D. (2018). Assessing changes in extreme river flow regulation from non-stationarity in hydrological scaling laws. *Journal of Hydrology*, *562*, 492–501.

Sáenz, L., Mulligan, M., Arjona, F., & Gutierrez, T. (2014). The role of cloud forest restoration on energy security. *Ecosystem Services*, *9*, 180–190.

Salazar, A., Sanchez, A., Villegas, J. C., Salazar, J. F., Ruiz Carrascal, D., Sitch, S., ... others (2018). The ecology of peace: preparing Colombia for new political and planetary climates. *Frontiers in Ecology and the Environment*, *16*(9), 525–531.

Salazar, J. F., Villegas, J. C., Rendón, A. M., Rodríguez, E., et al. (2018). Scaling properties reveal regulation of river flows in the Amazon through a "forest reservoir". *Hydrology and Earth System Sciences*, *22*(3), 1735–1748.

Setegn, S. G., Srinivasan, R., Melesse, A. M., & Dargahi, B. (2010). Swat model application and prediction uncertainty analysis in the lake tana basin, ethiopia. *Hydrological Processes: An International Journal*, *24*(3), 357–367.

Strauch, M., & Volk, M. (2013). SWAT plant growth modification for improved modeling of perennial vegetation in the tropics. *Ecological Modelling*, *269*, 98–112.

Suescún, D., Villegas, J. C., León, J. D., Flórez, C. P., García-Leoz, V., & Correa-Londono, G. A. (2017). Vegetation cover and rainfall seasonality impact nutrient loss via runoff

and erosion in the Colombian Andes. *Regional environmental change*, *17*(3), 827–839.
Tan, M. L., Gassman, P., Yang, X., & Haywood, J. (2020). A Review of SWAT Applications, Performance and Future Needs for Simulation of Hydro-Climatic Extremes. *Advances in Water Resources*, 103662.
Tapasco, J., Quintero, M., Uribe, N., Valencia, J., Calderón, S., Romero, G., … Ludeña, C. E. (2015). *Impactos económicos del cambio climático en Colombia: recurso hídrico* (Tech. Rep.). Washington, D.C.: Banco Interamericano de Desarrollo. Monografía No. 257.
Tian, F., Lü, Y. H., Fu, B. J., Zhang, L., Zang, C. F., Yang, Y. H., & Qiu, G. Y. (2017). Challenge of vegetation greening on water resources sustainability: Insights from a modeling-based analysis in Northwest China. *Hydrological processes*, *31*(7), 1469–1478.
Tobón, C., Bruijnzeel, L., Frumau, K. A., & Calvo-Alvarado, J. (2010). Changes in soil physical properties after conversion of tropical montane cloud forest to pasture in northern Costa Rica. *Tropical montane cloud forests: Science for conservation and management*, 502–515.
Uribe, N., Corzo, G., Quintero, M., van Griensven, A., & Solomatine, D. (2018). Impact of conservation tillage on nitrogen and phosphorus runoff losses in a potato crop system in Fuquene watershed, Colombia. *Agricultural Water Management*, *209*, 62–72.
Uribe, N., Srinivasan, R., Corzo, G., Arango, D., & Solomatine, D. (2020). Spatio-temporal critical source area patterns of runoff pollution from agricultural practices in the Colombian Andes. *Ecological Engineering*, *149*, 105810.
Urrea, V., Ochoa, A., & Mesa, O. (2019). Seasonality of Rainfall in Colombia. *Water Resources Research*, *55*(5), 4149–4162.
Verbesselt, J., Hyndman, R., Newnham, G., & Culvenor, D. (2010). Detecting trend and seasonal changes in satellite image time series. *Remote sensing of Environment*, *114*(1), 106–115.
Villamizar, S. R., Pineda, S. M., & Carrillo, G. A. (2019). The Effects of Land Use and Climate Change on the Water Yield of a Watershed in Colombia. *Water*, *11*(2), 285.
Viviroli, D., Dürr, H. H., Messerli, B., Meybeck, M., & Weingartner, R. (2007). Mountains of the world, water towers for humanity: Typology, mapping, and global significance. *Water resources research*, *43*(7).
Viviroli, D., Kummu, M., Meybeck, M., Kallio, M., & Wada, Y. (2020). Increasing dependence of lowland populations on mountain water resources. *Nature Sustainability*, 1–12.
Wagner, P., Kumar, S., Fiener, P., & Schneider, K. (2011). Hydrological modeling with SWAT in a monsoon-driven environment: experience from the Western Ghats, India. *Transactions of the ASABE*, *54*(5), 1783–1790.
Williams, J., Jones, C., Kiniry, J., & Spanel, D. A. (1989). The EPIC crop growth model. *Transactions of the ASAE*, *32*(2), 497–0511.
Yang, W., Long, D., & Bai, P. (2019). Impacts of future land cover and climate changes on runoff in the mostly afforested river basin in north China. *Journal of hydrology*, *570*, 201–219.
Ye, W., van Dijk, A. I., Huete, A., & Yebra, M. (2021). Global trends in vegetation seasonality in the gimms ndvi3g and their robustness. *International Journal of Applied Earth Observation and Geoinformation*, *94*, 102238.
Zemp, D. C., Schleussner, C.-F., Barbosa, H. M., Hirota, M., Montade, V., Sampaio, G., … Rammig, A. (2017). Self-amplified Amazon forest loss due to vegetation-atmosphere feedbacks. *Nature communications*, *8*(1), 1–10.
Zhang, H., Wang, B., Li Liu, D., Zhang, M., Leslie, L. M., & Yu, Q. (2020). Using an improved SWAT model to simulate hydrological responses to land use change: a case study of a catchment in tropical Australia. *Journal of Hydrology*, 124822.
Zhang, M., Liu, N., Harper, R., Li, Q., Liu, K., Wei, X., … Liu, S. (2017). A global review on hydrological responses to forest change across multiple spatial scales: Importance of scale, climate, forest type and hydrological regime. *Journal of Hydrology*, *546*,

44–59.
Zhang, X., Friedl, M. A., & Schaaf, C. B. (2006). Global vegetation phenology from moderate resolution imaging spectroradiometer (modis): Evaluation of global patterns and comparison with in situ measurements. *Journal of Geophysical Research: Biogeosciences*, *111*(G4).

Supporting Information for "SWAT-Tb with improved LAI representation in the tropics highlights the role of forests in watershed regulation"

Santiago Valencia[1], Juan F. Salazar[1], Juan Camilo Villegas[2], Natalia Hoyos[3], Mateo Duque-Villegas[1,4,5]

[1]GIGA, Escuela Ambiental, Facultad de Ingeniería, Universidad de Antioquia, Medellín, Colombia

[2]Grupo en Ecología Aplicada, Escuela Ambiental, Facultad de Ingeniería, Universidad de Antioquia, Medellín, Colombia

[3]Department of History and Social Sciences, Universidad del Norte, Barranquilla 080001, Colombia

[4]Max Planck Institute for Meteorology, Hamburg, Germany

[5]International Max Planck Research School on Earth System Modelling, Hamburg, Germany

Contents

Supplementary Material S1: SWAT-Tb implementation

Alemayehu, Griensven, Woldegiorgis, and Bauwens (2017) modified SWAT by adding two parameters (based on Strauch and Volk (2013)) that represent the end of the dry season (SOS1) and the beginning of the wet season (SOS2). In SWAT-Tb, we added three new parameters (SOS3, SOS4, and SOS5) to represent the seasonality of precipitation characterized by a bimodal regime with two wet and dry seasons. In this case, SOS1 and SOS2 represent the months of the end and beginning of the first dry-wet season transition, respectively. SOS3 represents the end of the first wet season and the beginning of the second dry season (i.e. a new growth cycle), whereas SOS4 and SOS5 indicate, respectively, the first and last month of the second dry-wet season transition. In SWAT-T, SOS1 and SOS2 parameters are estimated using the seasonal pattern of SMI based on precipitation and a reference evapotranspiration ratio (Figure 2; Alemayehu et al., 2017). The SOS(1,2,3,4,5) parameters are defined using mean monthly precipitation and LAI seasonality for each land cover category in the CR watershed.

Implementation of SWAT-Tb requires the user to add the lines shown below to the *allocate_parm.f, getallo.f, grow.f, modparm.f, readsub.f*, and *zero.f* subroutines from SWAT-T (Alemayehu et al., 2017). New lines are annotated as [svalencia]. The SWAT-Tb executable as well as the *.sub, *.mgt, and subroutines files, which must be adapted, are available online at `https://bit.ly/2XT8uxs`. This link is intended only to allow detailed revision of the manuscript. After publication, we may change the link to keep the files permanently available.

allocate_parm.f

```
  ! allocate tropical plant growth variables [talemayehu]
allocate (iseason(mhru))
allocate (sos1(msub))
allocate (sos2(msub))
```

```
allocate (sos3(msub)) !! Added by [svalencia]
allocate (sos4(msub)) !! Added by [svalencia]
allocate (sos5(msub)) !! Added by [svalencia]
```

getallo.f

```
  read (27,6100) subfile
call caps(subfile)
open (25,file=subfile)
do j = 1, 57 !! changed (54) [svalencia]
read (25,6000) titldum
end do
```

grow.f

```
  !!    INCOMING VARIABLES
!! sos1(:) |month |starting month of transition to first wet season added by [talemayehu]
!! sos2(:) |month |ending month of transition to first wet season added by [talemayehu]
!! added by [svalencia]
!! sos3(:) |month |ending of the first wet season and the starting of the second dry season
!! sos4(:) |month |starting month of transition to second wet season
!! sos5(:) |month |ending month of transition to second wet season


  if (smi_tr <=0.0) smi_tr = 0.5
idp = idplt(j)
```

```
if (Abs(sub_lat(hru_sub(j))) < 20. .AND.
iseason(j) == 0 .AND.
& i_mo >= sos1(hru_sub(j)) .AND.
& i_mo <= sos2(hru_sub(j))) then
smi=0.

  if (count_D(j)>0) then
do kk = 1, w_size-1
pet_subA(w_size-kk+1,(j)) = pet_subA(w_size-kk,(j))
end do
pet_subA(1,(j)) = pet_sub((j))
else
pet_subA(1,(j)) = pet_sub((j))
end if
if (count_D(j) > 0) then
do kk = 1, w_size-1
sub_pcpA(w_size-kk+1,(j)) =
& sub_pcpA(w_size-kk,(j))

  end do
sub_pcpA(1,(j)) = sub_pcp(hru_sub(j))
else
sub_pcpA(1,hru_sub(j)) = sub_pcp(hru_sub(j))
```

```
end if
count_D(j) = count_D(j) +1
if(count_D(j) > w_size) count_D(j) = w_size
if(count_D(j) == w_size) then
smi = sum(sub_pcpA(:,(j)))/sum(pet_subA(:,(j)))
if (smi >= smi_tr) then
call changeseason
count_D(j) = 0
end if

  end if
if(count_D(j) < w_size) then
smi = 0.0
end if
else if (Abs(sub_lat(hru_sub(j))) < 20. .AND.
& iseason(j) == 0 .AND. i_mo > sos2(hru_sub(j))
.AND. i_mo <= sos3(hru_sub(j))) then !! Added by [svalencia]
call changeseason
count_D(j) = 0

  !! Added by [svalencia]
else if (Abs(sub_lat(hru_sub(j))) < 20.
.AND. iseason(j) == 1 .AND.
```

```
& i_mo >= sos4(hru_sub(j)) .AND.
& i_mo <= sos5(hru_sub(j))) then
smi=0.

  if (count_D(j)>0) then
do kk = 1, w_size-1
pet_subA(w_size-kk+1,(j)) = pet_subA(w_size-kk,(j))
end do
pet_subA(1,(j)) = pet_sub((j))
else
pet_subA(1,(j)) = pet_sub((j))
end if
if (count_D(j) > 0) then
do kk = 1, w_size-1
sub_pcpA(w_size-kk+1,(j)) =
& sub_pcpA(w_size-kk,(j))

  end do
sub_pcpA(1,(j)) = sub_pcp(hru_sub(j))
else
sub_pcpA(1,hru_sub(j)) = sub_pcp(hru_sub(j))
end if
count_D(j) = count_D(j) + 1
```

```
if(count_D(j) > w_size) count_D(j) = w_size
if(count_D(j) == w_size) then

  smi = sum(sub_pcpA(:,(j)))/sum(pet_subA(:,(j)))
if (smi >= smi_tr) then
call changeseason
count_D(j) = 0
end if
end if
if(count_D(j) < w_size) then
smi = 0.0
end if

  else if (Abs(sub_lat(hru_sub(j))) < 20. .AND.
& iseason(j) == 0 .AND. i_mo > sos5(hru_sub(j))) then
call changeseason
count_D(j) = 0
end if
```

modparm.f

```
  !! added for plant growth modification for tropics added by [talemayehu]
integer, dimension (:), allocatable :: iseason, sos1, sos2, sos3, sos4, sos5 !! last three added by [svalencia]
```

readsub.f

```
read (101,*) sos1(i) !! added by [talemayehu]
read (101,*) sos2(i) !! added by [talemayehu]
read (101,*) sos3(i) !! added by [svalencia]
read (101,*) sos4(i) !! added by [svalencia]
read (101,*) sos5(i) !! added by [svalencia]
```

zero0.f

```
!!initialize tropical plant growth variables added by [talemayehu]
iseason = 0
sos1 = 0
sos2 = 0
sos3 = 0 !! added by [svalencia]
sos4 = 0 !! added by [svalencia]
sos5 = 0 !! added by [svalencia]
smi_tr = 0.
```

Supplementary material S2: Leaf Area Index (LAI) data and calibration

LAI data were obtained from the MCD15A2H-MODIS product (Myneni et al., 2015) for the GR watershed with a spatial and temporal resolution of 0.5 km and 8-days (composites), respectively. Only pixels with a corresponding "best quality" flag (LAI_QC=0) were kept for the analysis. We processed LAI data following methods used in Alemayehu et al. (2017) and Hoyos et al. (2019). For most land cover types, LAI values were extracted as follows: (i) polygons with an area at of least 5 km^2 within the CR watershed are selected for each land cover, (ii) LAI values are associated to each land cover type only in pixels where such land cover type covers at least 60% of the area. For shrubs (RYEB) and planted forest (PINE), which cover less than 12% of the CR watershed, polygons are smaller than 5 km^2. Therefore, the corresponding LAI values were extracted from polygons in the vicinity of the CR watershed, within the GR watershed. Median LAI values for each land cover type and period (8-day composites) were calculated from the aforementioned polygons as suggested by Strauch and Volk (2013) and Alemayehu et al. (2017).

For the LAI calibration, the initial values of parameters such as the initial (LAI_INIT), minimum (ALAI_MIN) and maximum (BLAI) LAI values for each land cover type were set based on the long-term MODIS-LAI time series (Figure 3 and Supplementary Figure S1). Initial values of Plant Heat Units (PHU) were calculated using the long-term daily mean temperature, as suggested by Strauch and Volk (2013). Other initial parameters were defined based on literature (e.g., T_BASE, T_OPT, CHTMX, and CANMX; see Table S2) and default values (e.g., FRGW1, FRGW2, LAIMX1, LAIMX2, and DLAI). These parameters were calibrated by a trial-and-error process to ensure that the LAI values simulated by SWAT-T and SWAT-Tb mimicked the smoothed MODIS-LAI. The Pearson correlation coefficient (r), the percent of bias (PBIAS), and the Kling–Gupta efficiency (KGE) (Gupta et al., 2009) were used to evaluate the agreement between simulated and observation-based estimates (MODIS) of LAI.

References

Alemayehu, T., Griensven, A. v., Woldegiorgis, B. T., & Bauwens, W. (2017). An improved SWAT vegetation growth module and its evaluation for four tropical ecosystems. *Hydrology and Earth System Sciences*, *21*(9), 4449–4467.

Cárdenas Agudelo, M. F., et al. (2016). *Ecohydrology of paramos in Colombia: Vulnerability to climate change and land use* (Unpublished doctoral dissertation). Universidad Nacional de Colombia-Sede Medellín.

Cook, B., Pengelly, B., Brown, S., Donnelly, J., Eagles, D., Franco, M., ... Peters, M. (2005). *Schultze-Kraft; R. 2005. Tropical Forages: an interactive selection tool,[CD-ROM].* CSIRO, DPIetF (Qld), CIAT and ILRI, Brisbane, Australia.

García-Leoz, V., Villegas, J. C., Suescún, D., Flórez, C. P., Merino-Martín, L., Betancur, T., & León, J. D. (2017). Land cover effects on water balance partitioning in the Colombian Andes: improved water availability in early stages of natural vegetation recovery. *Regional Environmental Change*, 1–13.

González-Orozco[1], C. E., Jarvis, A., & Palacio, J. D. (2011). Predicting the climatic distribution of the Colombian oak Quercus humboldtii Bonpl.(Fagaceae). *Novedades Colombianas*, *11*, 1–17.

Gupta, H. V., Kling, H., Yilmaz, K. K., & Martinez, G. F. (2009). Decomposition of the mean squared error and NSE performance criteria: Implications for improving hydrological modelling. *Journal of hydrology*, *377*(1-2), 80–91.

Hofstede, R. G., Castillo, M. X. M., & Osorio, C. M. R. (1995). Biomass of grazed, burned, and undisturbed páramo grasslands, Colombia. I. Aboveground vegetation. *Arctic and Alpine Research*, *27*(1), 1–12.

Hoyos, N., Correa-Metrio, A., Jepsen, S. M., Wemple, B., Valencia, S., Marsik, M., ... Velez, M. I. (2019). Modeling Streamflow Response to Persistent Drought in a Coastal Tropical Mountainous Watershed, Sierra Nevada De Santa Marta, Colombia. *Water*, *11*(1), 94.

Jaramillo-Robledo, A. (2003). La lluvia y el transporte de nutrimentos dentro de ecosistemas de bosque y cafetales. *Cenicafé*, *54*(2), 134–144.

Leguizamon, J. V., & Marín, C. T. (2017). Influencia de la vegetación en el funcionamiento hidrológico de cuencas de humedales de alta montaña tropical. *Revista Ecosistemas*, *26*(2), 10–17.

Moriasi, D. N., Arnold, J., Van Liew, M. W., Bingner, R. L., Harmel, R. D., & Veith, T. L. (2007). Model evaluation guidelines for systematic quantification of accuracy in watershed simulations. *Transactions of the ASABE*, *50*(3), 885–900.

Myneni, R., Knyazikhin, Y., & Park, T. (2015). *MCD15A2H MODIS/Terra+ Aqua Leaf Area Index/FPAR 8-day L4 Global 500 m SIN Grid V006, NASA EOSDIS Land Processes DAAC.*

Orwa, C., Mutua, A., Kindt, R., Jamnadass, R., Simons, A., et al. (2009). Agroforestree Database: a tree reference and selection guide. Version 4. *Agroforestree Database: a tree reference and selection guide. Version 4.*.

Peters, M., Franco, T., Schmidt, A., & Hincapié Carvajal, B. (2011). *Especies forrajeras multipropósito: Opciones para productores del Trópico Americano.* Centro Internacional de Agricultura Tropical (CIAT); Bundesministerium für . . . .

Spracklen, D. V., & Righelato, R. (2016). Carbon storage and sequestration of re-growing montane forests in southern Ecuador. *Forest Ecology and Management*, *364*, 139–144.

Strauch, M., & Volk, M. (2013). SWAT plant growth modification for improved modeling of perennial vegetation in the tropics. *Ecological Modelling*, *269*, 98–112.

Veneklaas, E. J., & Van Ek, R. (1990). Rainfall interception in two tropical montane rain forests, Colombia. *Hydrological processes*, *4*(4), 311–326.

Table S1. Reclassification of land cover types in the CR watershed according to SWAT categories.

Land cover type	**SWAT category**	**Description**	**Area (%)**
Pasture	RYEL	Pasture dominated by *Pennisetum clandestinum Hochst, ex Chiow (Poaceae)*, used for cattle dairy	51.24
Native Andean forest	FRST	Forest dominated by mature Andean Oak (*Quercus humboldtii* Bonpl. Fagaceae)	29.30
Shrubs	RYEB	Secondary succession with little to no human intervention	11.42
Paramo vegetation	BROM	High altitude native grasslands with sparse vegetation cover and ocasional presence of shrubs	4.89
Pasture with secondary growth	RYEE	Unmanaged grasslands with occurrence of sparse secondary vegetation	2.93
Planted forest	PINE	Forest dominated by *Pinus patula* Schltdl. Cham	0.09

Table S2. LAI-ralated parameters for each land cover type and their initial and calibrated values in the SWAT-Tb model.

Parameter	Description	Calibrated values (initial values)					
		FRST	**RYEL**	**RYEB**	**RYEE**	**BROM**	**PINE**
LAI_INIT[1]	Initial leaf area index (m^2/m^2)	4.20* (4.17)	1.80* (1.90)	3.50* (3.74)	2.30 (-)	3.10* (3.16)	3.60* (3.80)
BIO_INIT	Initial dry weight biomass (kg/ha)	50000[2] (-)	20000[3] (-)	20000 (-)	20000 (-)	20000[4] (-)	50000 (-)
PHU_PLT[5]	Total number of heat units or growing degree days needed to bring plant to maturity	3000* (1700)	3000* (1700)	1700 (-)	1800* (1700)	2000 (-)	5000 (-)
BLAI[1]	Maximum potential leaf area index (m^2/m^2)	4.40* (3.79)	1.95* (1.68)	4.50* (3.22)	2.80* (2.0)	3.20* (2.62)	3.90* (3.50)
ALAI_MIN[1]	Minimum leaf area index (m^2/m^2)	2.60* (3.38)	1.25* (1.35)	1.85* (1.44)	1.45* (1.41)	2.0* (1.19)	2.0* (2.70)
FRGRW1	Fraction of PHU corresponding to the 1st point on the leaf area development curve	0.15* (0.05)	0.10* (0.20)	0.07* (0.20)	0.07* (0.20)	0.07* (0.45)	0.10* (0.15)
FRGRW2	Fraction of PHU corresponding to the 2nd point on the leaf area development curve	0.38* (0.40)	0.40* (0.45)	0.20* (0.45)	0.40* (0.45)	0.20* (0.80)	0.38* (0.25)
LAIMX1	Fraction of BLAI corresponding to the 1st point on the optimal leaf area development curve	0.70* (0.05)	0.10* (0.32)	0.15* (0.32)	0.10* (0.32)	0.15* (0.02)	0.40* (0.70)
LAIMX2	Fraction of BLAI corresponding to the 2nd point on the optimal leaf area development curve	0.90* (0.95)	0.99* (0.95)	0.99* (0.95)	0.99* (0.95)	0.99* (0.95)	0.90* (0.99)
DLAI	Fraction of PHU when LAI beings to decline	0.20* (0.99)	0.99* (0.50)	0.5** (-)	0.99* (0.50)	0.85** (-)	0.99* (-)
T_BASE	Minimum temperature for plant growth (∘C)	9.30[6] (-)	0* (7.0[7])	9.30[7] (-)	9.30[7] (-)	7.0* (4.0[8])	0* (10.0[7])
T_OPT	Optimal temperature for plant growth (∘C)	18.60[6] (-)	18.0[7] (-)	18.6[6] (-)	18.60[6] (-)	18.0* (10.0[8])	14.0[7] (-)
BIO_E	Radiation use efficiency ((kg/ha)/(MJ/m^2))	18.0* (15.0)	10.0* (30.0)	10.0* (30.0)	10.0* (30.0)	15.0* (35.0)	10.0* (15.0)
CHTMX	Maximum canopy height (m)	25.0[9] (-)	0.30[3,10] (-)	1.20[10] (-)	1.20[10] (-)	0.50[8] (-)	25.0[9] (-)
CANMX	Maximum canopy storage (mm H_2O)	0.30[11,12](-)	0.05[10](-)	0.20[10,12](-)	0.05[10,12](-)	0.15[13](-)	0.10(-)
BMDIEOFF	Biomass die-off fraction	0.1 ** (-)	0.05** (0.1)	0.1** (-)	0.1**(-)	0.1*(-)	0.1*(-)
SOS1[14]	First month of the 1st dry-wet season transition	3 (-)					
SOS2[14]	Last month of the 1st dry-wet season transition	4 (-)					
SOS3[14]	End of first wet season and the beginning of second dry season	6 (7)					
SOS4[14]	First month of the 2nd dry-wet season transition	10 (9)					
SOS5[14]	Last month of the 2nd dry-wet season transition	11 (10)					

FRST: native Andean forest, RYEL: pasture, RYEB: shrubs, RYEE: pasture with secondary growth, BROM: paramo vegetation, PINE: planted forest.[1]BFAST-MODIS LAI time series; *Manual adjustment during calibration process; **Default values in SWAT; [2]Spracklen and Righelato (2016); [3]Peters, Franco, Schmidt, and Hincapié Carvajal (2011); [4]Hofstede, Castillo, and Osorio (1995); [5]Initial values estimated from local temperature records following Strauch and Volk (2013) and other studies (Hoyos et al., 2019); [6]González-Orozco[1], Jarvis, and Palacio (2011); [7]Cook et al. (2005); [8]Cárdenas Agudelo et al. (2016); [9]Orwa et al. (2009); [10]García-Leoz et al. (2017); [11]Veneklaas and Van Ek (1990);[12]Jaramillo-Robledo (2003);[13]Leguizamon and Marín (2017);[14] Parameters determined using LAI filtered data, precipitation seasonality, and manual LAI calibration.

Table S3. Global sensitivity analysis in the SWAT-Tb model. Sensitivity is indicated by a high t-statistic value (in absolute terms) and a low p-value. Parameters are listed from high to low sensitivity.

Parameter[1]	Description	Scaling type[2]	Range Min	Range Max	t-statistic	p-value
CN2.mgt_RYEL	Runoff curve number for moisture condition II	r	-0.25	0.25	-16.989	0.000
ESCO.hru_RYEL	Soil evaporation compensation factor	v	0.01	1	-9.989	0.000
ESCO.hru_FRST	Soil evaporation compensation factor	v	0.01	1	-8.197	0.000
ALPHA_BF.gw	Baseflow alpha factor (1/days)	v	0.01	1	-7.299	0.000
CN2.mgt_FRST	Runoff curve number for moisture condition II	r	-0.25	0.25	-6.280	0.000
SOL_K(1).sol_RYEL	Saturated hydraulic conductivity (mm/hr)	r	-0.50	0.50	-4.802	0.000
GWQMN.gw_FRST	Threshold depth of water in the shallow aquifer required for return flow to occur (mm H_2O)	v	0	5000	4.669	0.000
CH_K2.rte	Effective hydraulic conductivity in main channel alluvium (mm/hr)	v	0	150	4.428	0.000
GWQMN.gw_RYEL	Threshold depth of water in the shallow aquifer required for return flow to occur (mm H_2O)	v	0	5000	3.996	0.000
ESCO.hru_BPRR	Soil evaporation compensation factor	v	0.01	1	-3.314	0.001
SOL_K(1).sol_FRST	Saturated hydraulic conductivity (mm/hr)	r	-0.50	0.50	-3.158	0.002
SOL_BD(1).sol_BPRR	Moist bulk density (g/cm^3)	r	-0.20	0.20	-2.902	0.004
CN2.mgt_BPRR	Runoff curve number for moisture condition II	r	-0.25	0.25	-2.774	0.006
SOL_AWC(1).sol_FRST	Available water capacity of the soil layer (mm H_2O/mm soil)	r	-0.50	0.50	-2.599	0.009
SOL_BD(1).sol_RYEL	Moist bulk density (g/cm^3)	r	-0.20	0.20	-2.468	0.014
GWQMN.gw_BPRR	Threshold depth of water in the shallow aquifer required for return flow to occur (mm H_2O)	v	0	5000	-2.399	0.017
SOL_K(1).sol_BPRR	Saturated hydraulic conductivity (mm/hr)	r	-0.50	0.50	-2.238	0.026
SOL_AWC(1).sol_RYEL	Available water capacity of the soil layer (mm H_2O/mm soil)	r	-0.50	0.50	-1.950	0.050
SOL_K(2).sol_RYEL	Saturated hydraulic conductivity (mm/hr)	r	-0.50	0.50	-1.867	0.062
SOL_BD(2).sol_BPRR	Moist bulk density (g/cm^3)	r	-0.20	0.20	-1.770	0.077
SOL_BD(1).sol_FRST	Moist bulk density (g/cm^3)	r	-0.20	0.20	-1.607	0.109
SOL_K(2).sol_BPRR	Saturated hydraulic conductivity (mm/hr)	r	-0.50	0.50	-1.541	0.124
RCHRG_DP.gw	Deep aquifer percolation fraction	v	0	1	-1.527	0.128
SOL_AWC(2).sol_FRST	Available water capacity of the soil layer (mm H_2O/mm soil)	r	-0.50	0.50	-1.186	0.236
SOL_AWC(2).sol_RYEL	Available water capacity of the soil layer (mm H_2O/mm soil)	r	-0.50	0.50	-1.175	0.241
SOL_K(2).sol_FRST	Saturated hydraulic conductivity (mm/hr)	r	-0.50	0.50	-1.010	0.313
GW_DELAY.gw_RYEL	Groundwater delay times (days)	v	0.01	500	0.406	0.685
GW_DELAY.gw_FRST	Groundwater delay times (days)	v	0.01	500	-0.379	0.705
SOL_AWC(1).sol_BPRR	Available water capacity of the soil layer (mm H_2O/mm soil)	r	-0.50	0.50	0.354	0.723
GW_DELAY.gw_BPRR	Groundwater delay times (days)	v	0.01	500	0.309	0.758
SOL_AWC(2).sol_BPRR	Available water capacity of the soil layer (mm H_2O/mm soil)	r	-0.50	0.50	-0.170	0.865
SOL_BD(2).sol_FRST	Moist bulk density (g/cm^3)	r	-0.20	0.20	0.115	0.908
SOL_BD(2).sol_RYEL	Moist bulk density (g/cm^3)	r	-0.20	0.20	0.027	0.978

[1]Numbers (1, 2) refer to the soil layer number. Land cover types are native Andean forest (FRST), pasture (RYEL) and BPRR (paramo vegetation, planted forest, shrubs, and pasture with secondary growth). [2]Scaling type: v (absolute) indicates that the parameter is replaced by the given value, r (relative) indicates that the parameter is multiplied by [1 + (given value)].

Table S4. Comparison of SWAT average water flux components before and after calibration with reference values.

Model	SWAT average water flux components [1] (mm/yr)								Ratios		
	PREC	**SURQ**	**LATQ**	**GWQ**	**PET**	**ET**	**REVAP**	**WYLD**	**Baseflow ratio (GWQ/ WYLD)**	**Runoff ratio (SURQ/ WYLD)**	**ET ratio [(ET+REVAP)/ PREC]**
SWAT-T	1841.43	114.36	60.67	590.47	862.68	358.19	17.25	1464.77	0.40	0.07	0.20
SWAT-Tb (LAI calibration)	1841.43	96.52	46.28	401.03	862.68	747.19	17.25	1074.82	0.37	0.09	0.42
SWAT-Tb (LAI + streamflow calibration)	1841.43	16.72	49.88	319.97	862.68	838.80	17.25	954.23	0.33	0.02	0.46
Reference value									0.4-0.5[2]	0.04-0.16[3]	0.5-0.6[4]

Calibration period from 2003 to 2016.[1] PREC = precipitation, SURQ = surface runoff contribution to streamflow, LATQ = lateral flow contribution to streamflow, GWQ = grundwater contribution to streamflow, PET = potential evapotranspiration, ET = actual evapotranspiration, REVAP = amount of water moving from shallow aquifer to plants/soil profile, and WYLD = water yield. Reference values from: [2] baseflow filter (`https://engineering.purdue.edu/mapserve/WHAT/`), [3] Jaramillo-Robledo (2003), and [4] García-Leoz et al. (2017).

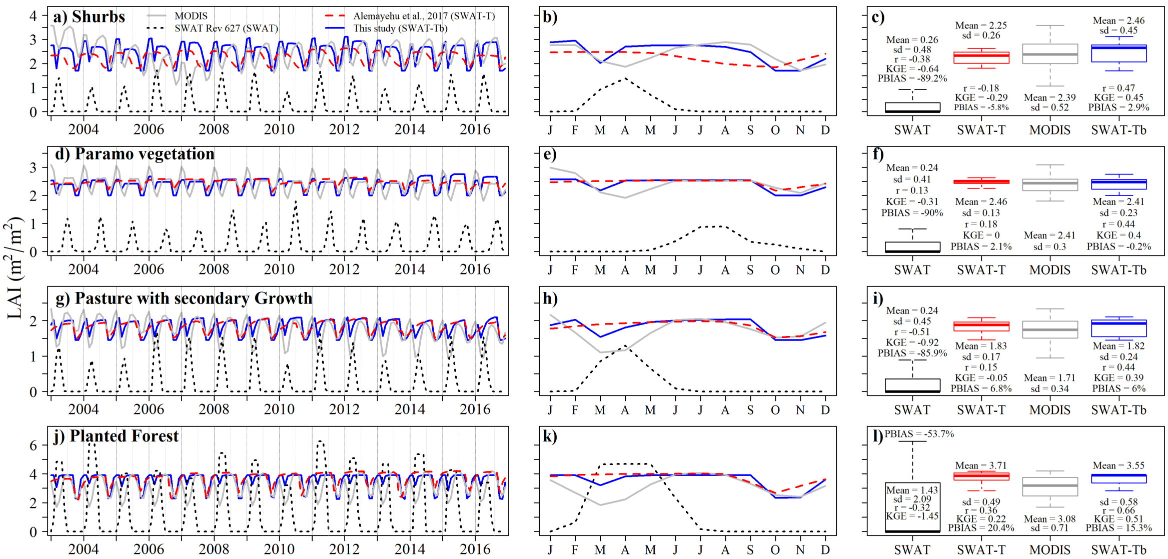

Figure S1. Observed (MODIS) and simulated (SWAT, SWAT-T, and SWAT-Tb) seasonality of LAI in the CR watershed for for (a-c) shrubs (RYEB), (d-f) paramo vegetation (BROM), (g-i) pasture with secondary growth (RYEE), and (j-k) planted forest (PINE). Time series (a,d,g,j), average annual cycle (b,e,h,k), and the (c,f,i,l) corresponding boxplots and performance statistics.

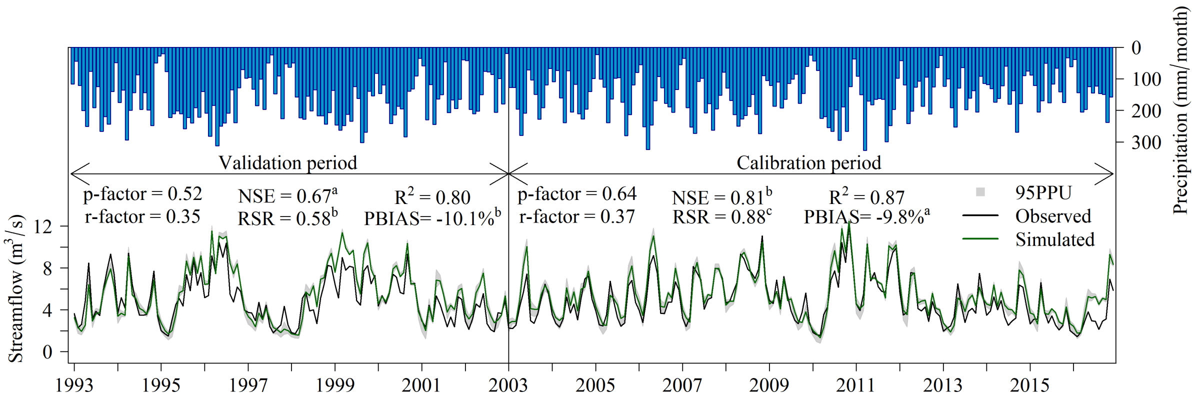

Figure S2. Calibration (2003–2016) and validation (1993–2002) of SWAT for monthly streamflow. Vertical bars show monthly rainfall from SWAT outputs, calculated from records in climate stations. Model performances based on the criteria of Moriasi et al. (2007): ^{a} Good (0.65<NSE≤0.75, 0.50<RSR≤0.60, ±10%<BIAS< ±15%) and ^{b} Very Good (0.75<NSE≤1.00, 0.00<RSR≤0.50, BIAS≤±10%).

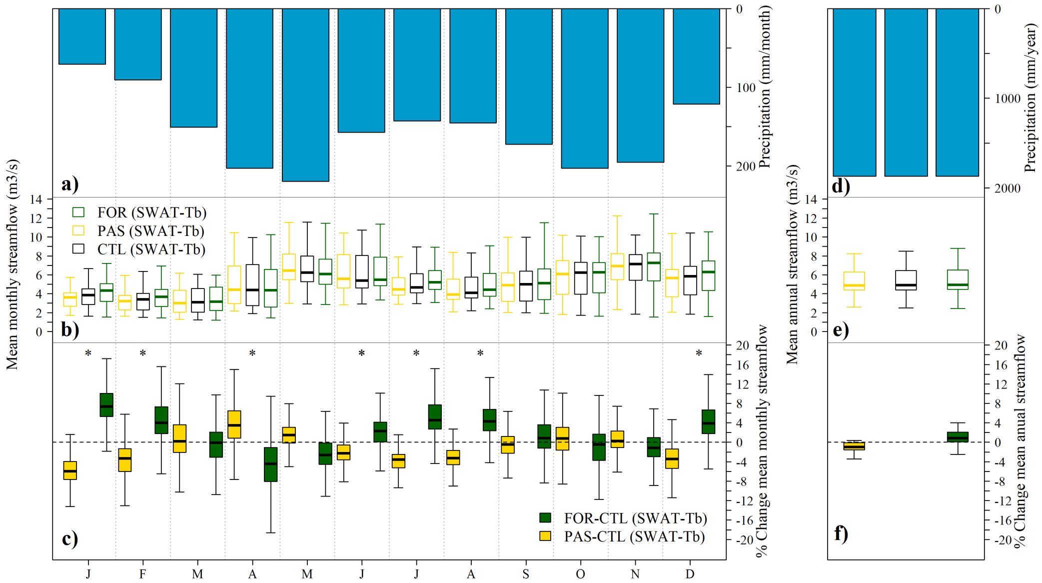

Figure S3. Comparison of monthly (left) and annual (right) streamflow between scenarios using 1000 simulations with parameters ranges as we did for the model calibration. Input precipitation (blue bars) is the same for all scenarios and models (a,d). Average seasonal cycle (b) and annual streamflow (e) in all scenarios for 1993–2016. Percent differences between monthly (c) and annual (f) streamflow in the control (CTL) and LULC (FOR and PAS) scenarios for 1993–2016 as simulated by SWAT-Tb and SWAT using best fit parameters. Positive (negative) values indicate that streamflow is increased (decreased) in the LULC change scenario. Asterisks identify months for which the difference between medians in the FOR and PAS scenarios is statistically significant (n=24000, $p < 0.05$) for SWAT-Tb output.